UNCLASSIFIED

AD NUMBER
ADA196950
LIMITATION CHANGES

TO:

Approved for public release; distribution is unlimited.

FROM:

Distribution authorized to U.S. Gov't. agencies and their contractors; Administrative/Operational Use; MAY 1987. Other requests shall be referred to European Research Office, 429 Oxford St, London.

AUTHORITY

ST-A PER DTIC FORM 50.

THIS PAGE IS UNCLASSIFIED

AD-A196 950

CHARACTERIZATION OF THE BACKGROUND NATURAL AEROSOL IN THE WEST OF IRELAND

S.G. JENNINGS
(Principal Investigator)
University College
Galway

CONTRACT NUMBER : DAJA45-87-C-0016

3rd Interim Report

May 1987

DTIC
S ELECTE D
JUN 2 8 1988
D

CHARACTERIZATION OF THE BACKGROUND NATURAL AEROSOL IN THE WEST OF IRELAND

This interim report describes

(i) Aerosol particle number and size distributions for ambient air at Mace Head Atmospheric Research Station, Carna in the West of Ireland about 50 miles west of Galway City.

(ii) Intercomparison of particle sizing instrumentation used by University College Galway and UMIST, Manchester.

(iii) Calculations of optical extinction and lidar backscatter to extinction ratios at predominantly laser wavelengths from the visible to middle-IR - based on measured aerosol particle size distributions.

(i)   Aerosol particle number and size distribution measurements at Mace Head.

Introduction

Use was made of a Particle Measuring Systems (PMS) Active Scattering Probe - ASASP-X probe.   The probe was realigned and calibrated for size response by means of polyvinyltoluene latex and polystyrene latex monodisperse spherical particles.   The size calibration agreed to within plus/minus one channel resolution of the manufacturers response, and is given in Table 1 below.

Table 1.   Size calibration of Particle Measuring Systems (PMS) ASASP-X light scattering counter.

	Range 3	Range 2	Range 1	Range 0
Particle diameter intervals (μm)	0.09-0.20	0.15-0.30	0.24-0.84	0.6-3.0

Field measurements have been carried out spanning both 1987 and the present year at about one monthly intervals.   A listing of the field test dates is given in Table 2.

Table 2.   Field Measurement Tests

Date	Prevaling Wind Direction	Comments
December 10 - 11, 1987	Easterly	2 s data throughout. Solenoid valves in operation.
December 16 - 17, 1987	Southerly	Some measurements bypassing solenoid valves were made.
January 13 - 15, 1988	South-westerly-westerly	2s data.
February 13 - 19, 1988	-	Intercalibration of particle sizing instrumentation at UMIST, Manchester.
March 10 - 12, 1988	Westerly	4 s data, no solenoid valves in use.
April 19 - 22, 1988	Southeasterly to southwesterly	Parallel measurements at Mace Head and at Great Dun Fell.

The ambient aerosol field measurements of December 10-11, 1987 were made
with a normally open solenoid valve in line to the ASASP-X probe.
Laboratory tests, using ammonium sulphate polydispersion of particles as a
test aerosol, were carried out to compare particle concentration passing
through the normally open valve with that passing directly to the sizing
probe.   Results of this comparison yielded averaged losses of 12.1%, 14%,
19.6% and 62.8% for ranges 3, 2, 1, 0.   These percentage losses are mainly
due to the presence of a sharp L shaped bend in the normally open valve.
Ambient aerosol particle concentration measurements made on December 10-11,
1987 were corrected by applying the above laboratory loss correction valves
to the data.   The rest of the ambient aerosol data presented was obtained
via direct access to the ASASP-X probe.

The aerosol particle size data was taken at 2 s intervals for the first
three field data sets.   Subsequent field data is taken at a 4 s interval.
Particle concentration is measured directly since the PMS ASASP-X is
totally plumbed i.e. each particle is counted as it traverses the laser
beam.   Hence particle concentration is known as accurately as the flow
rate through the particle counter.   Periodic flow calibration measurements
were performed in the laboratory.   A flow rate of 1 cm^3 s^{-1} was maintained
for all ambient aerosol measurements.

Analysis of the Aerosol Field Data

The aerosol particle data is presented here in two formats:

(i) Aerosol concentration per cm^3 as a function of particle radius.

(ii) Aerosol concentration per cm^3 per micron as a function of particle
     radius.

Format (i) tends to show 'spikes' which are due to overlapping size ranges
with larger number concentration than in neighbouring size channels of the

adjacent (lower) size range. These spikes are smoothed out using format (ii) where the particle concentration is weighted against the width of the particle channel.

The data is presented here in chronological order. Figure 1 and 2 show the uncorrected data of aerosol particle concentration per cc, per cc per micron as a function of particle radius for December 11, 1987. The corrected data, allowing for particle loss through the solenoid valve is shown in Figures 3 and 4. A relatively high particle concentration is noted for the easterly wind direction - corresponding to the source of the aerosol coming from the continental European landmass.

Additional ambient aerosol concentration data is presented in Fig.5 and 6 for Dec. 17, 1987 at Mace Head, for a predominantly southerly airstream, Fig. 7, Fig. 8, Fig. 9 and Fig. 10 shows particle size data for five minute periods on January 14th and 15th, 1988.

An intensive measurement period was also carried out for March 10th-11th, 1988. Data is presented firstly for four consecutive cycles of duration twenty five minutes over the time period 1805 through 2120. Figures 11, and 12 give consecutive cyclic particle concentration as a function of particle radius for both formats. An average of the four cycles data is given in Figs. 13 and 14. Similar data plots are shown in Figs. 15, 16, 17 and 18 for five consecutive data cycles of duration twenty five minutes over the time period 2230 through 0235, on March 10th and 11th, 1988. A more comprehensive analysis of these data sets will be performed for the final report. In addition, analysis will also be made of the data set of April 19-22, 1988 which forms a major part of the joint trajectory study carried out in parallel with the UMIST research group under the supervision of Dr. T. Choularton, at Great Dun Fell, over the same time period.

(ii) Intercomparison of particle sizing instrumentation used by University College Galway and UMIST, Manchester.

The PMS ASASP-X probe was brought to the Department of Pure and Applied Physics, UMIST, Manchester on February 18th 1988. Intercomparison was performed between the Galway ASASP-X probe and the UMIST ASASP probe. The inter-range compatibility of the two probes is shown in Table 3. The Galway ASASP-X was adopted as the standard probe since it measured particle number concentration absolutely. Laboratory generated polydispersion of ammonium sulphate were used as the test aerosol. Sequential measurements of particle number concentration of the ammonium sulphate aerosol were made using the ASASP-X and the ASASP probes. A detailed analysis of this comparison is ongoing and will be presented in the final report.

(iii) Calculation of optical extinction, and lidar backscatter based on the measured particle size distributions

A modified version of the Mie program of Dave (1963) was used for E-O scattering calculations in this work, under the simplifying assumption that all particles are homogeneous spheres.

The transmission of a monochromatic laser beam through an assemblage of particles is derived from the Lambert-Bouguer law. The extinction coefficient $\sigma_e(m^{-1})$ is determined from the measurement of the transmitted signal I after traversal through the assemblage of particles of path length L:

$$I = I_o \exp(-\sigma_e L) \qquad (1)$$

TABLE 3

The inter-range compatibility of the ASASX and ASASP

ASAS-X Range 0 = ASASP Range 0   Range 1

particle size	channnel		particle size	ASAS-X	ASASP
0.600-0.759	ch1		0.240-0.280	ch1	
0.750-0.919	ch2		0.280-0.320	ch2	
0.920-1.079	ch3		0.320-0.360	ch3	
1.080-1.239	ch4		0.360-0.400	ch4	
1.240-1.399	ch5		0.400-0.440	ch5	ch1
1.400-1.559	ch6		0.440-0.480	ch6	ch2
1.560-1.719	ch7		0.480-0.520	ch7	ch3
1.720-1.879	ch8		0.520-0.560	ch8	ch4
1.880-2.039	ch9		0.560-0.600	ch9	ch5
2.040-2.199	ch10		0.600-0.640	ch10	ch6
2.200-2.359	ch11		0.640-0.680	ch11	ch7
2.360-2.519	ch12		0.680-0.720	ch12	ch8
2.520-2.679	ch13		0.720-0.760	ch13	ch9
2.680-2.839	ch14		0.760-0.800	ch14	ch10
2.840-3.000	ch15		0.800-0.840	ch15	ch11
			0.840-0.880		ch12
			0.880-0.920		ch13
			0.920-0.960		ch14
			0.960-1.000		ch15

ASAS-X Range 2 = ASASP Range 3

particle size	channel
0.15-0.16	ch1
0.16-0.17	ch2
0.17-0.18	ch3
0.18-0.19	ch4
0.19-0.20	ch5
0.20-0.21	ch6
0.21-0.22	ch7
0.22-0.23	ch8
0.23-0.24	ch9
0.24-0.25	ch10
0.25-0.26	ch11
0.26-0.27	ch12
0.27-0.28	ch13
0.28-0.29	ch14
0.29-0.30	ch15

ASAS-X sample volume   1 cc/sec

ASASP sample volume   0.105 cc/sec

∴ multiplication factor = 9.52

where I_0 is the initial intensity of the laser radiation in the absence of particles.

The volume extinction and backscatter coefficients σ_e and σ_b of a polydispersion of spherical particles characterized by a size distribution n(r) and refractive index m are given by

$$\sigma_e = \int \pi r^2 Q_e n(r) dr, \qquad (2)$$

$$\sigma_b = \frac{1}{4\pi} \int \pi r^2 G n(r) dr, \qquad (3)$$

where $Q_e(m,x)$ is the Mie efficiency factor for extinction for a particle with refractive index m and size parameter $x = 2\pi r/\lambda$, and $G(m,x)$ is the backscatter gain defined as 4π times the ratio of the backscatter differential cross section to the geometric area.

Refractive index values were chosen to represent the more commonly found atmospheric constituents for maritime aerosol: sodium chloride and ammonium sulphate. Refractive index values for these two constituents for visible to middle infrared wavelengths are given in Table 4. Also shown in Table 4 are calculated values of total extinction coefficient (m^{-1}) based on the averaged measured particle size distribution data of March 10th-11th, 1988 over the time period 2230-0235 (see Fig.18).

Table 4. Extinction coefficient (m^{-1}) for visible up to middle IR wavelengths based on measured particle size distributions (Fig. 18) at Mace Head, on March 10-11, 1988.

SODIUM CHLORIDE

WAVELENGTH (µm)	REFRACTIVE INDEX	TOTAL EXTINCTION COEFFICIENT (m^{-1})
0.55	$1.548-1.0\times10^{-7}$ i	2.25×10^{-5}
0.6934	$1.542-1.0\times10^{-7}$ i	2.27×10^{-5}
1.06	$1.53 -1.0\times10^{-7}$ i	2.06×10^{-5}
3.8	$1.513-1.0\times10^{-7}$ i	5.89×10^{-6}
10.6	$1.49 -1.0\times10^{-7}$ i	1.82×10^{-7}

AMMONIUM SULPHATE

WAVELENGTH (µm)	REFRACTIVE INDEX	TOTAL EXTINCTION COEFFICIENT (m^{-1})
0.55	$1.52-1.0\times10^{-7}$ i	2.26×10^{-5}
0.6934	$1.52-1.0\times10^{-7}$ i	2.26×10^{-5}
1.06	$1.51-2.4\times10^{-6}$ i	2.05×10^{-5}
3.8	$1.56-.02$ i	7.19×10^{-6}
10.6	$1.99-.06$ i	1.025×10^{-6}

The calculations were made for the visible wavelength of 0.55 um together for the wavelengths corresponding to the laser lines 0.6934, 1.06, 3.8 and 10.6 µm. Calculations of the total backscatter coefficient (m^{-1} sr^{-1}) for the same data set and for the same five wavelengths are given in Table 5 for the constituents of sodium chloride and ammonium sulphate.

The differential extinction coefficient (per m per micron) is plotted in Fig. 19 as a function of particle radius based on the averaged particle

Table 5. Backscatter coefficient (m^{-1} sr^{-1}) for visible up to middle IR wavelengths based on measured particle size distributions (Fig. 18) at Mace Head, on March 10-11, 1988.

SODIUM CHLORIDE

WAVELENGTH (μm)	REFRACTIVE INDEX	TOTAL EXTINCTION COEFFICIENT (m^{-1} sr^{-1})
0.55	$1.548-1.0 \times 10^{-7}$ i	2.48×10^{-6}
0.6934	$1.542-1.0 \times 10^{-7}$ i	2.42×10^{-6}
1.06	$1.53 -1.0 \times 10^{-7}$ i	1.49×10^{-6}
3.8	$1.518-1.0 \times 10^{-7}$ i	1.025×10^{-7}
10.6	$1.49 -1.0 \times 10^{-7}$ i	1.69×10^{-8}

AMMONIUM SULPHATE

WAVELENGTH (μm)	REFRACTIVE INDEX	TOTAL EXTINCTION COEFFICIENT (m^{-1} sr^{-1})
0.55	$1.52-1.0 \times 10^{-7}$ i	1.86×10^{-6}
0.6934	$1.52-1.0 \times 10^{-7}$ i	1.98×10^{-6}
1.06	$1.51-2.4 \times 10^{-6}$ i	1.20×10^{-6}
3.8	$1.56-.02$ i	1.017×10^{-7}
10.6	$1.99-.06$ i	5.31×10^{-8}

size distribution data of four cycles for March 10th, 1805 through 2120 (shown in Fig. 14). The particles are assumed to be comprised of ammonium sulphate. The calculations are for wavelength 0.55 μm (uppermost curve) through to 10.6 μm (lowest curve). A similar plot is shown in Fig.20 for sodium chloride particles. Figures 21 and 22 show calculated values of the differential backscatter coefficient (per m per steradian per micron) as a function of particle radius for the same data set.

Calculated values of the differential extinction coefficient (per m per micron) as a function of particle radius are shown in Fig. 23 and 24 for ammonium sulphate and sodium chloride particles based on the averaged values of particle size distribution measured over five cycles for the March 10th-11th, 1988, 2230 through 0235 (see Fig. 18). Figures 25 and 26 give the differential backscatter coefficient as a function of particle radius for the same data set.

Finally, the extinction to backscatter ratio calculated for each of the particle probe size channels at wavelengths 0.55, 0.6934, 1.06, 3.8 and 10.6 μm are plotted in Fig. 27 and Fig. 28 for constituents ammonium sulphate and sodium chloride. One can see that the extinction to backscatter ratio approach constant values for the visible to near infrared wavelengths but have resonant values at the larger middle IR wavelengths.

REFERENCES

Davé, J.V., Report No. 320-3237, IBM Scientific Center, Palo Alto, California (1968).
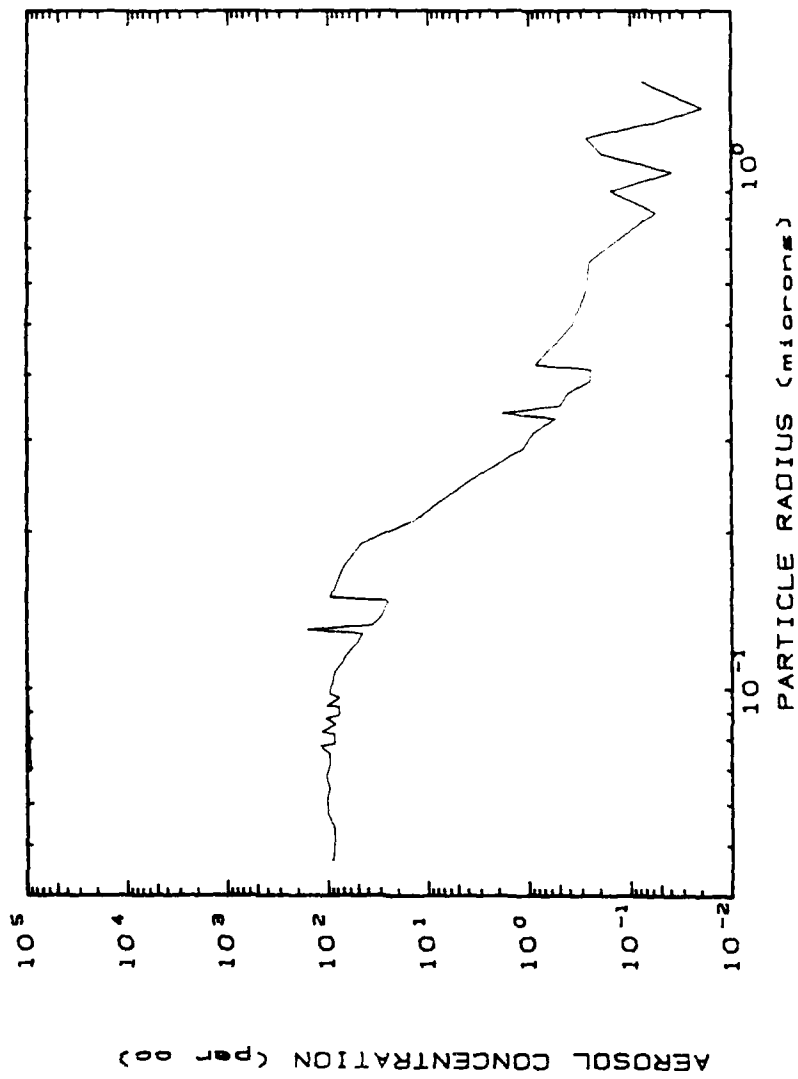
Fig. 1   Aerosol particle concentration per cc as a function of particle radius, (uncorrected). Mace Head, 11 Dec. 1987. Time: 0330-0911. Wind direction: easterly.
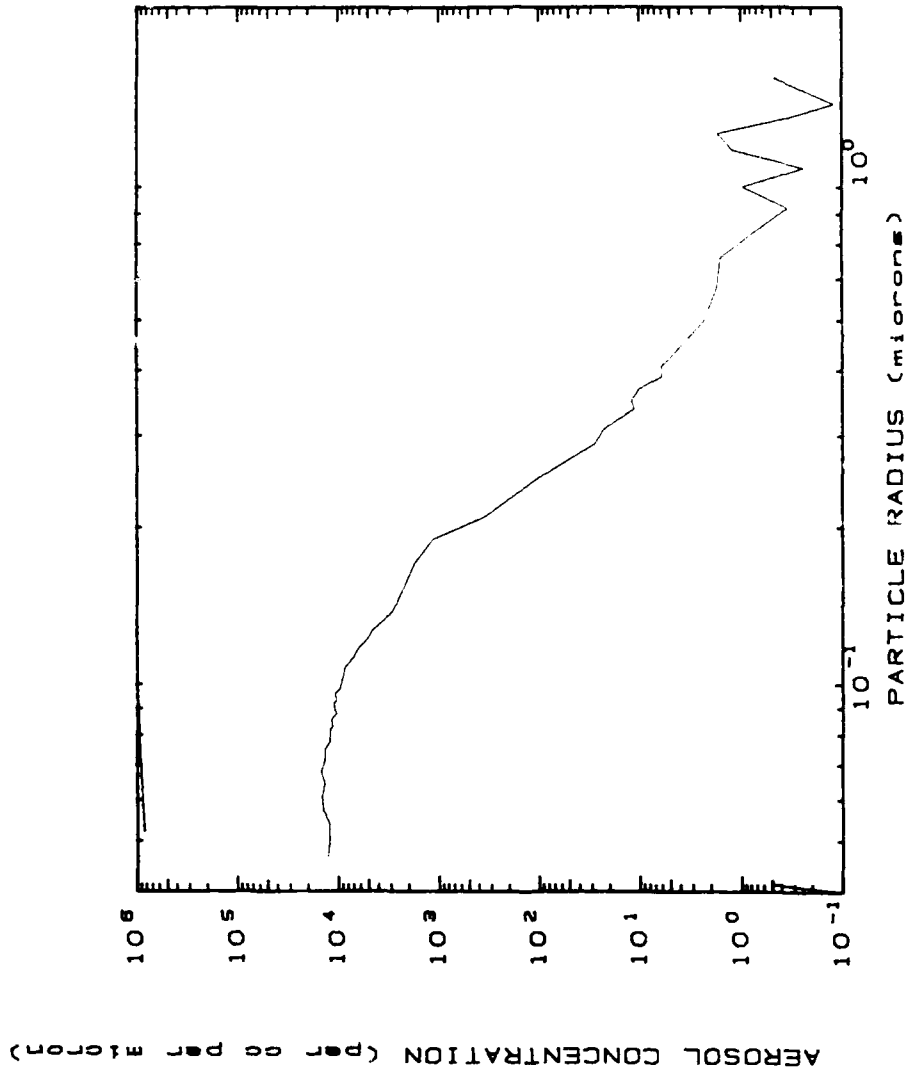
Fig. 2.   Aerosol particle concentration per cc per micron as a function of particle radius, (uncorrected).
Mace Head, 11 Dec. 1987.   Time 0330-0911.   Wind direction: easterly.
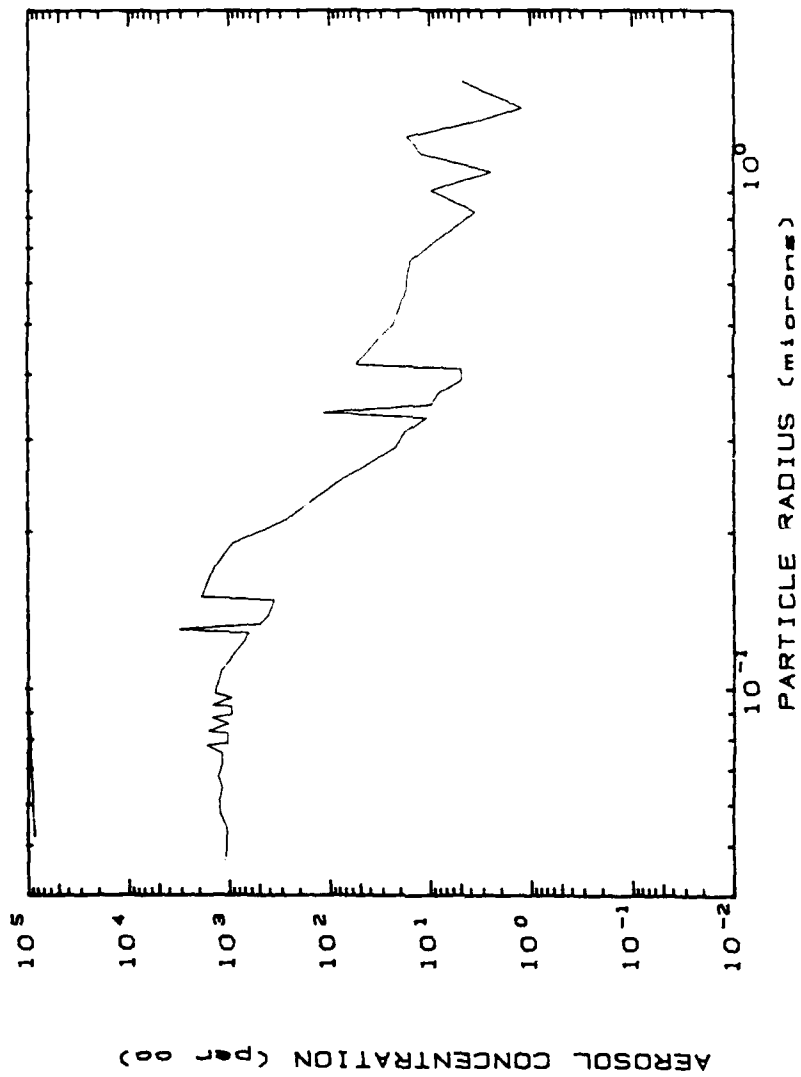
Fig. 3. Aerosol particle concentration per cc as a function of particle radius, (corrected). Mace Head, 11 Dec. 1987. Time: 0330-0911. Wind direction: easterly.
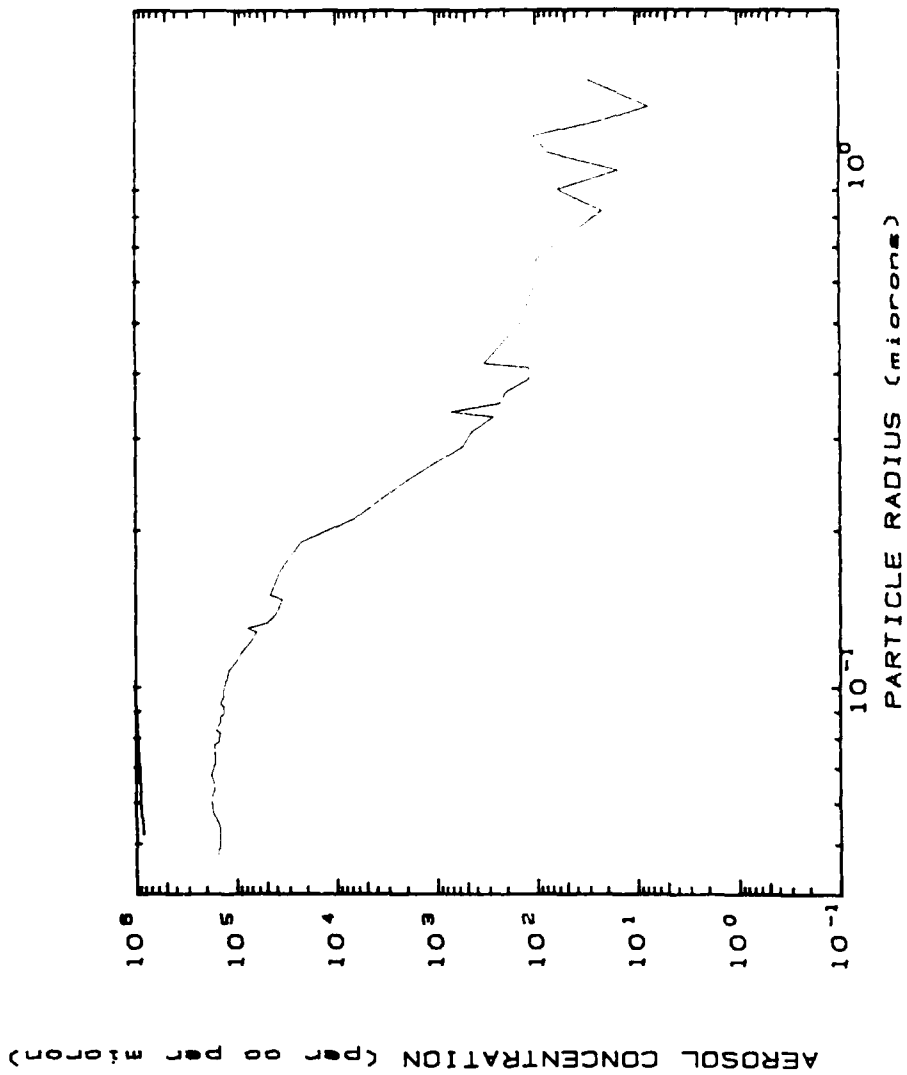
Fig. 4. Aerosol particle concentration per cc per micron as a function of particle radius, (corrected).
Mace Head, 11 Dec. 1987. Time: 0330-0911. Wind direction: easterly.

Fig. 5. Aerosol particle concentration per cc as a function of particle radius.
Mace Head, 17 Dec. 1987.   Time: 1511-1516 (upper curve); 1431-1436 (lower curve)
Wind direction: southerly.
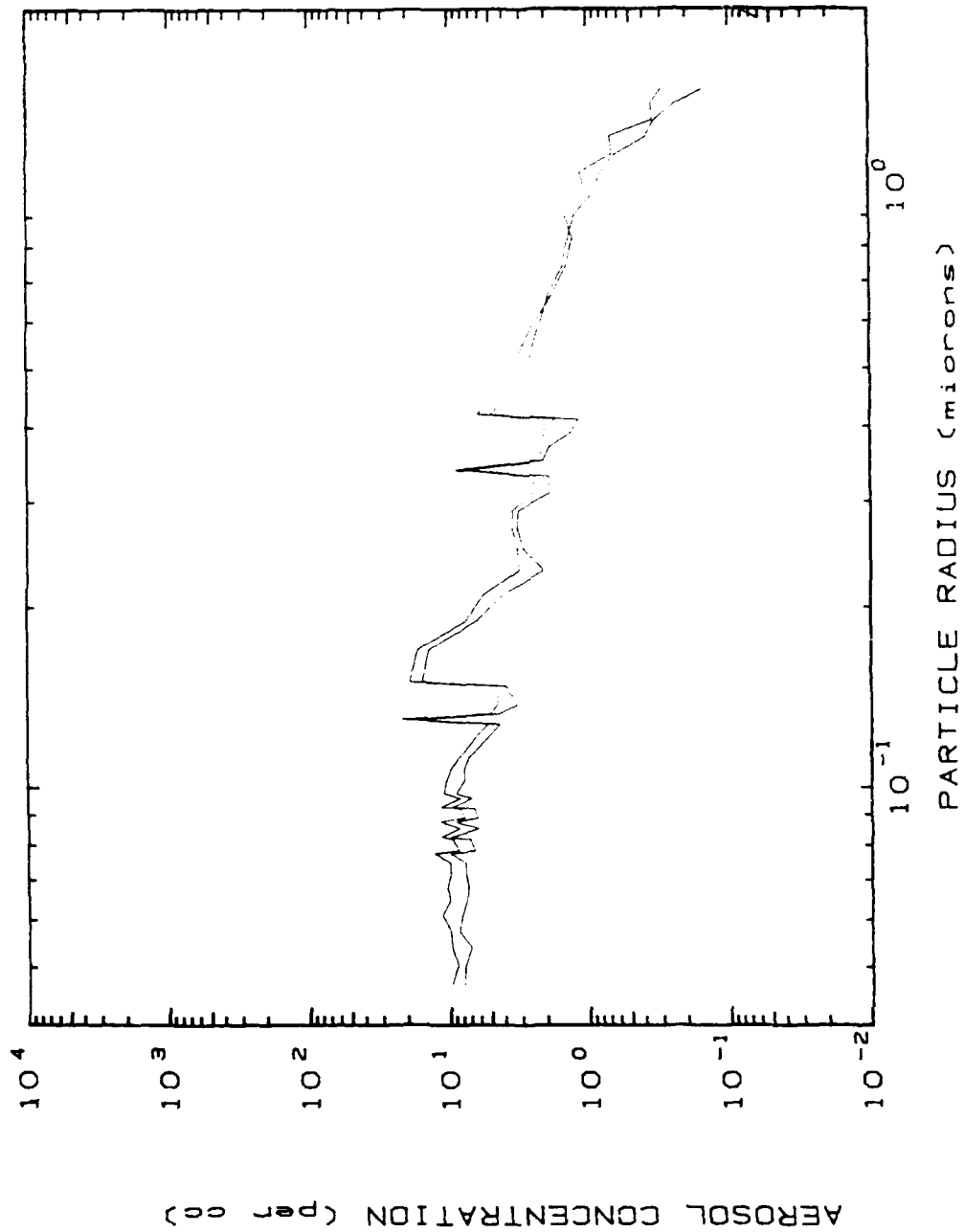
PARTICLE RADIUS (microns)

AEROSOL CONCENTRATION (per cc per micron)
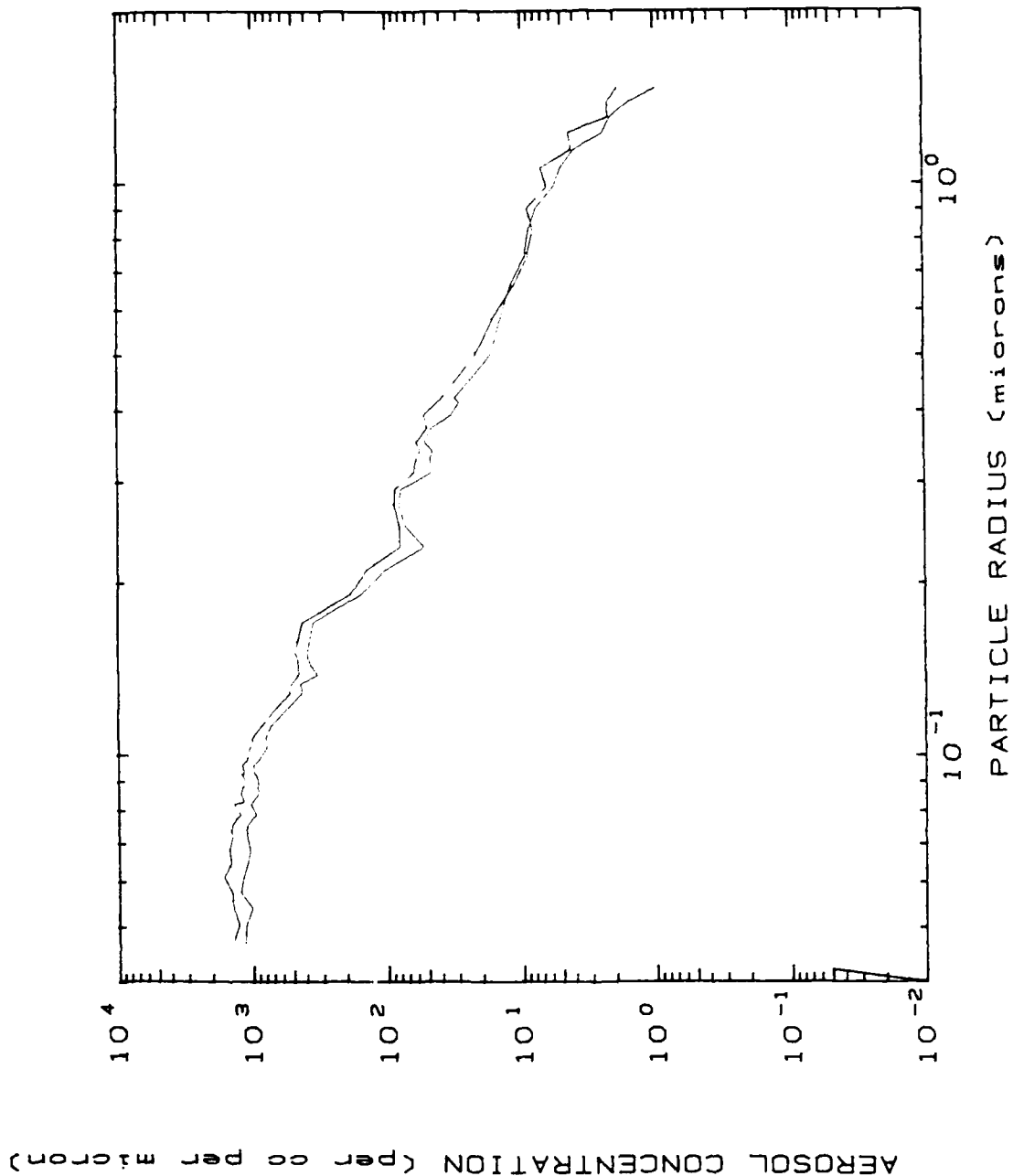
Fig. 6. Aerosol particle concentration per cc per micron as a function of particle radius. Mace Head, 17 Dec. 1987. Time: 1511-1516 (upper curve); 1431-1436 (lower curve). Wind direction: southerly.

Fig. 7. Aerosol particle concentration per cc as a function of particle size.
Mace Head 14 January 1988. Time 1140-1145. Wind direction: south westerly.

PARTICLE RADIUS (microns)
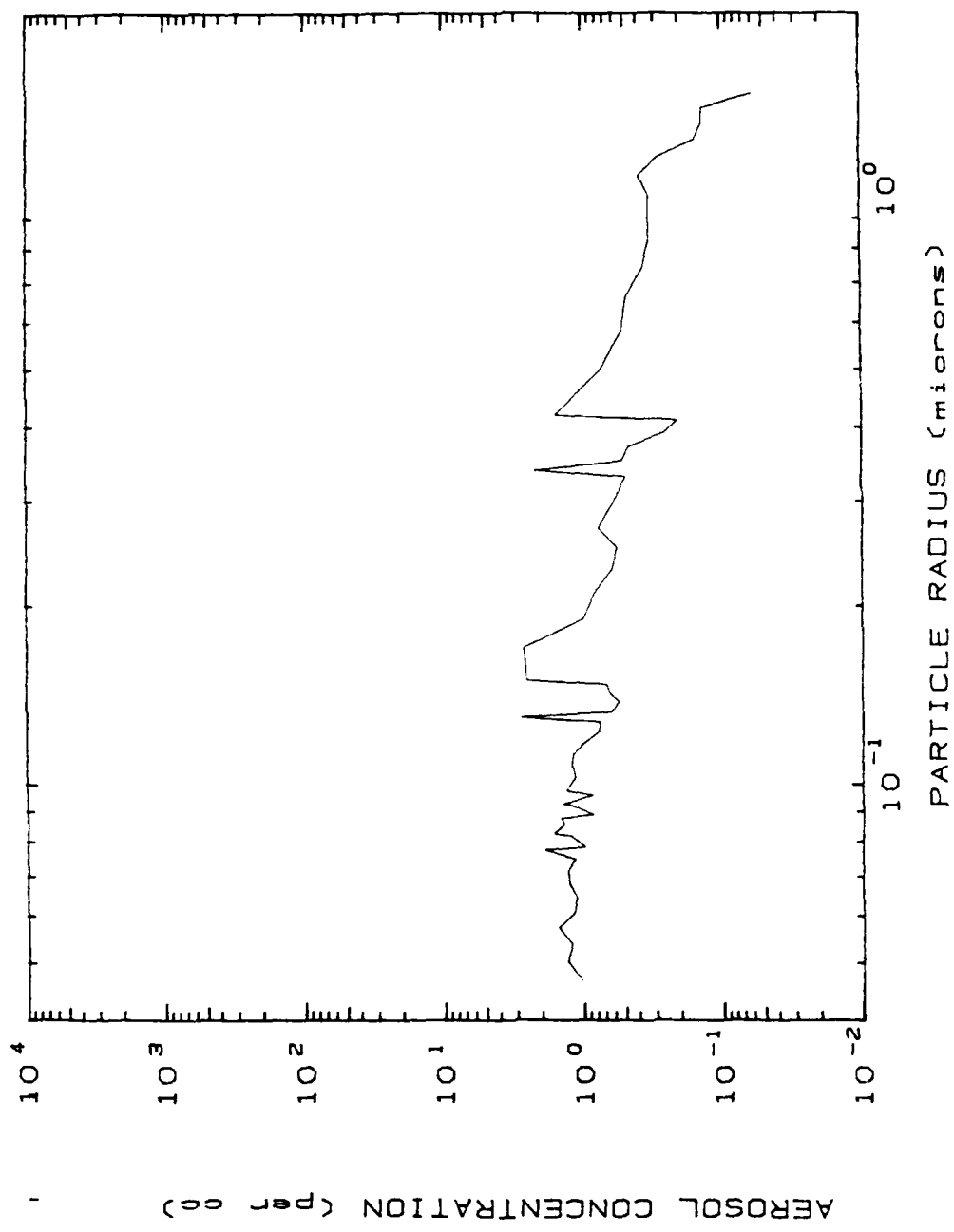
AEROSOL CONCENTRATION (per cc per micron)
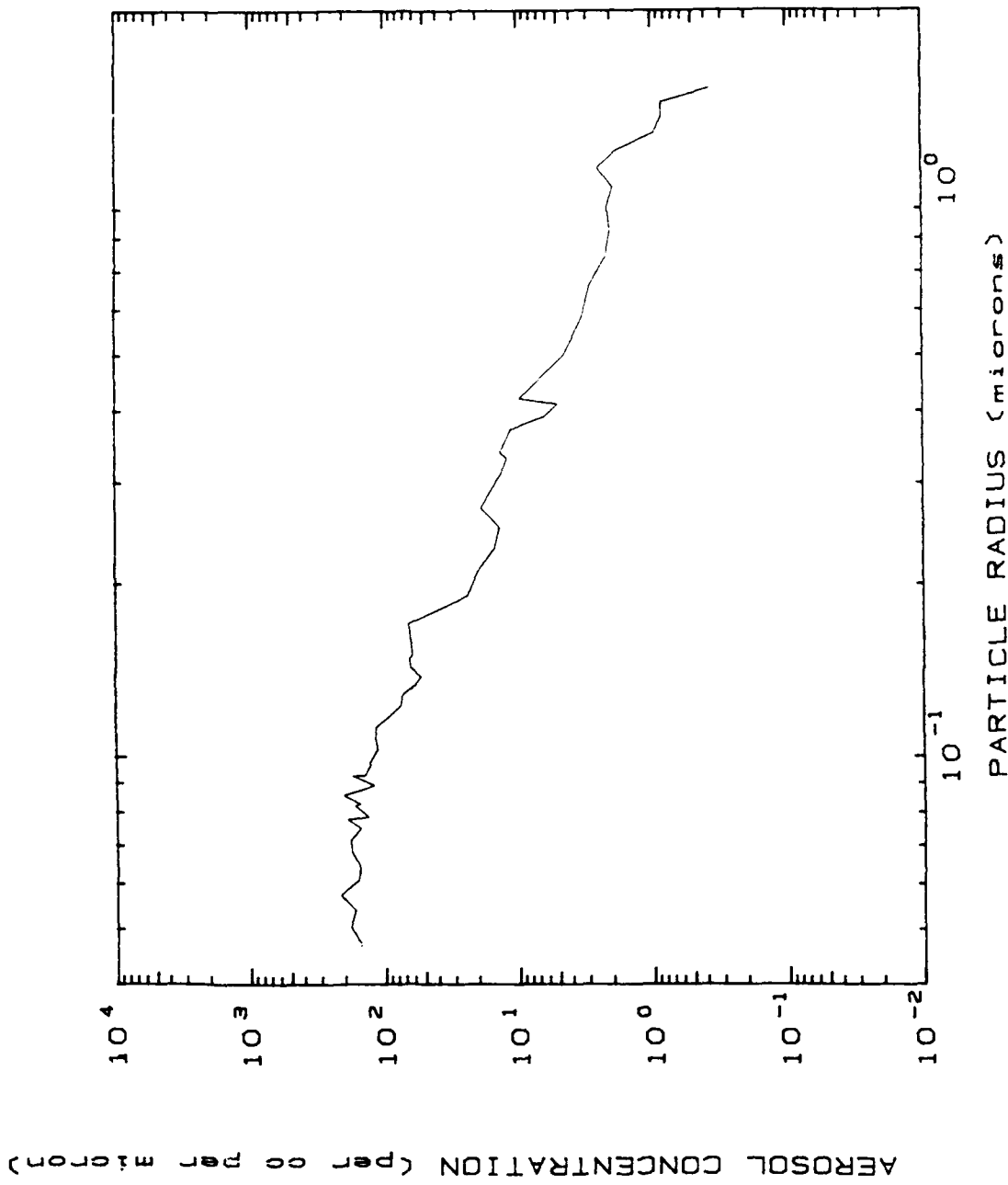
Fig. 8. Aerosol particle concentration per cc per micron as a function of particle size. Mace Head 14 January 1988. Time 1140-1145. Wind direction: south westerly.

Fig. 9. Aerosol particle concentration per cc as a function of particle radius.
Mace Head, 15 January 1988. Time: 0038-0043. Wind direction: south westerly.
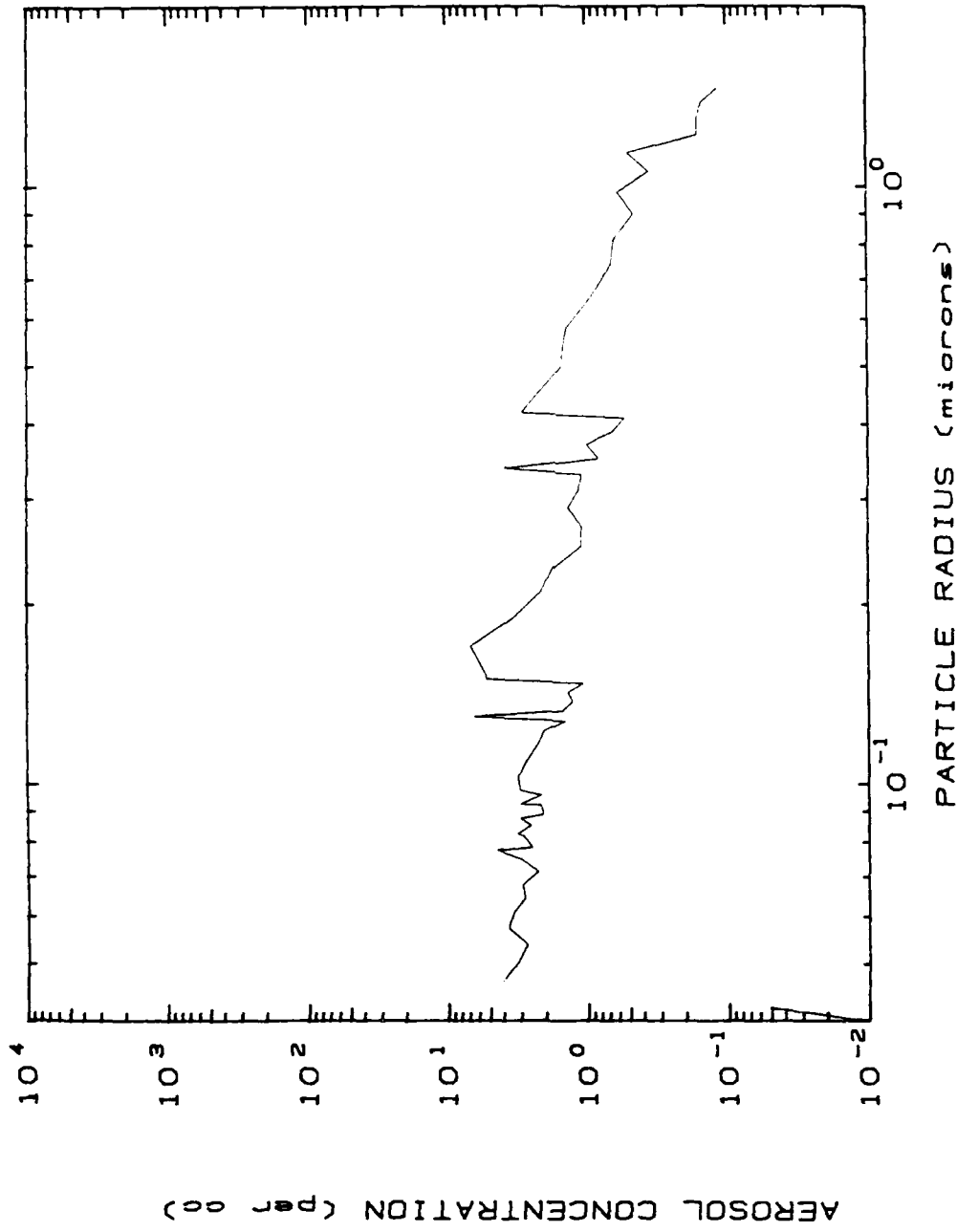
PARTICLE RADIUS (microns)

AEROSOL CONCENTRATION (per cc per micron)
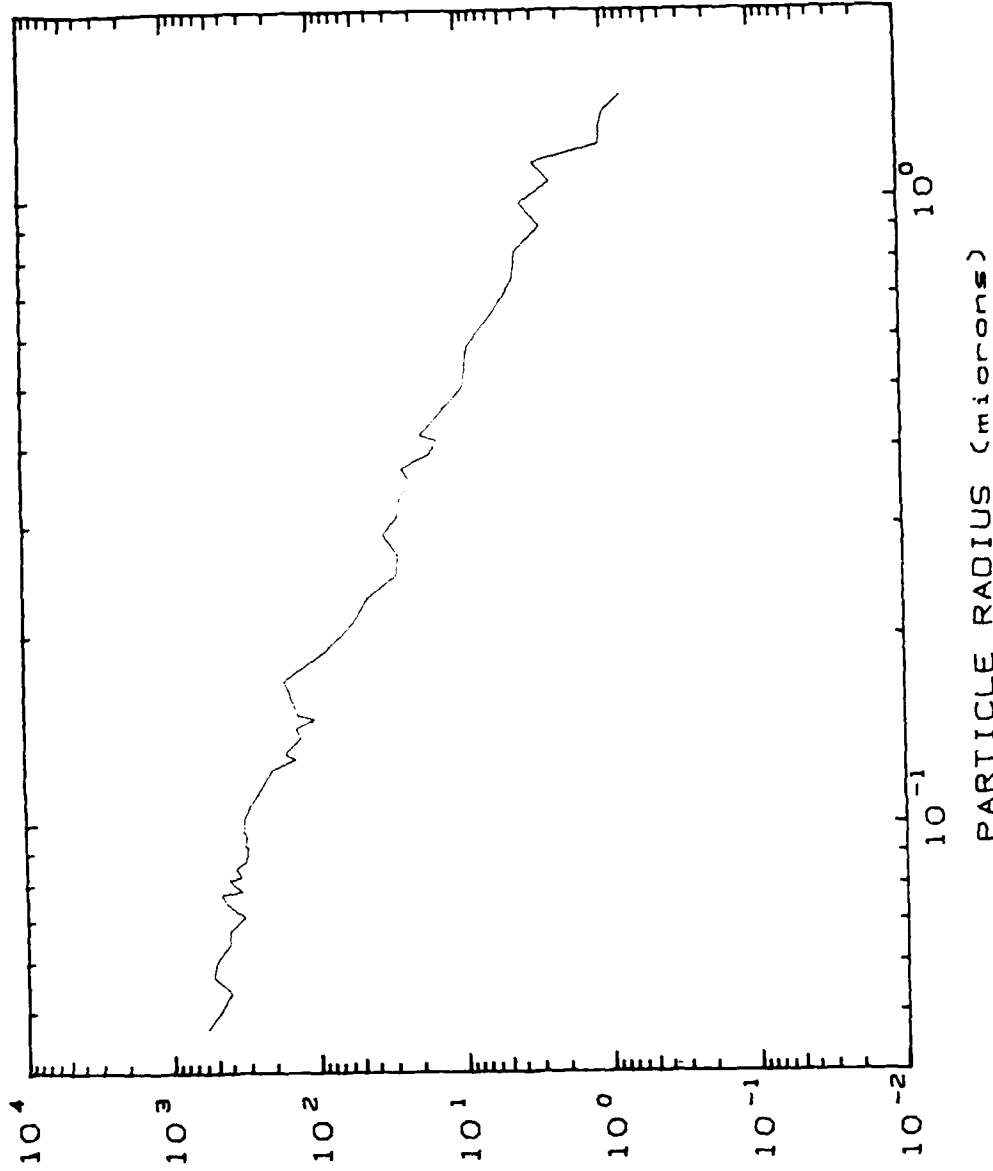
Fig. 10. Aerosol particle concentration per cc per micron as a function of particle radius. Mace Head, 15 January 1988. Time: 0038-0043. Wind direction: south westerly.
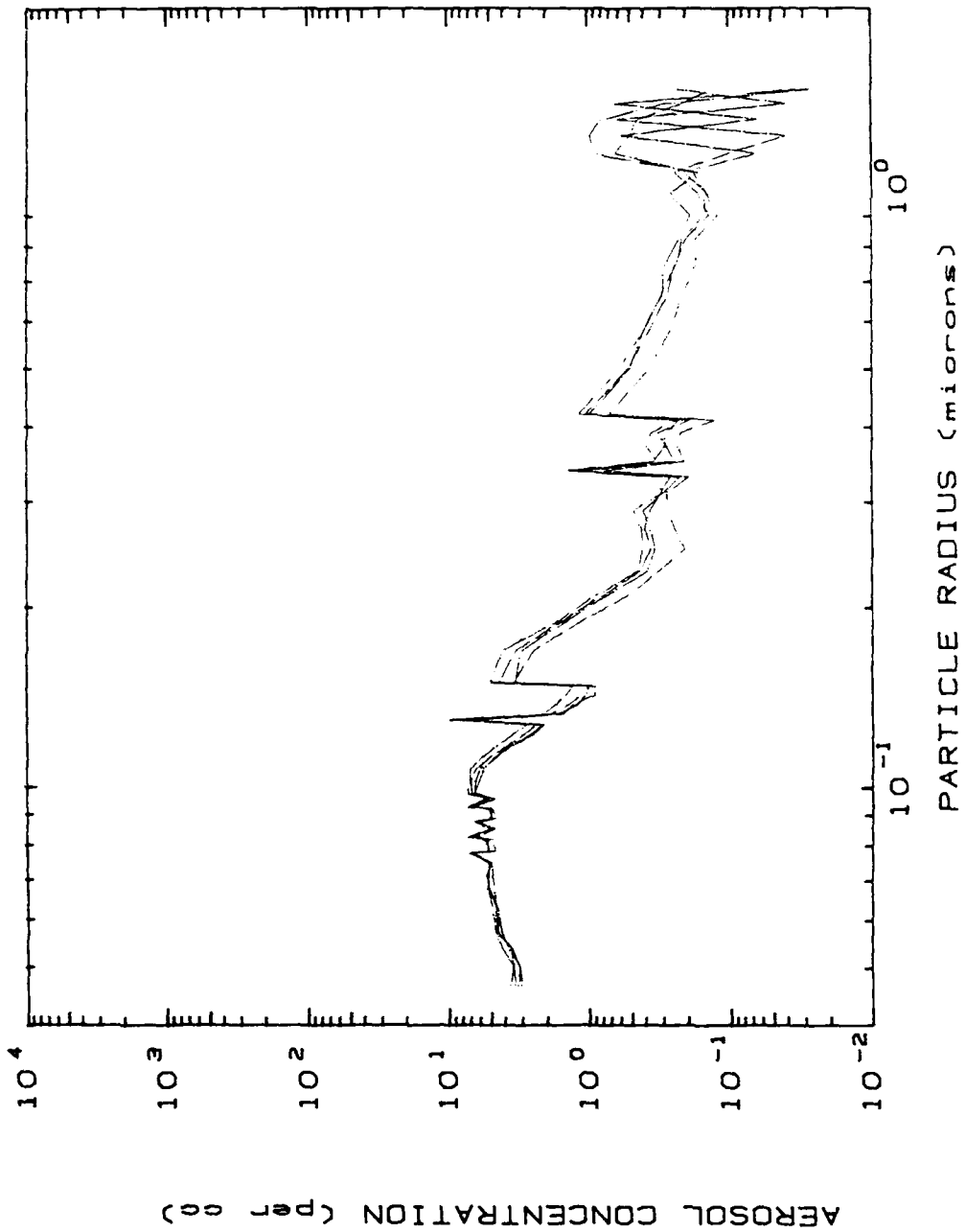
Fig. 11. Four consecutive data cycles of particle number concentration per cc as a function of particle radius.
Mace Head, 10 March 1988.   Time: 1805-2120.   Wind direction: westerly.
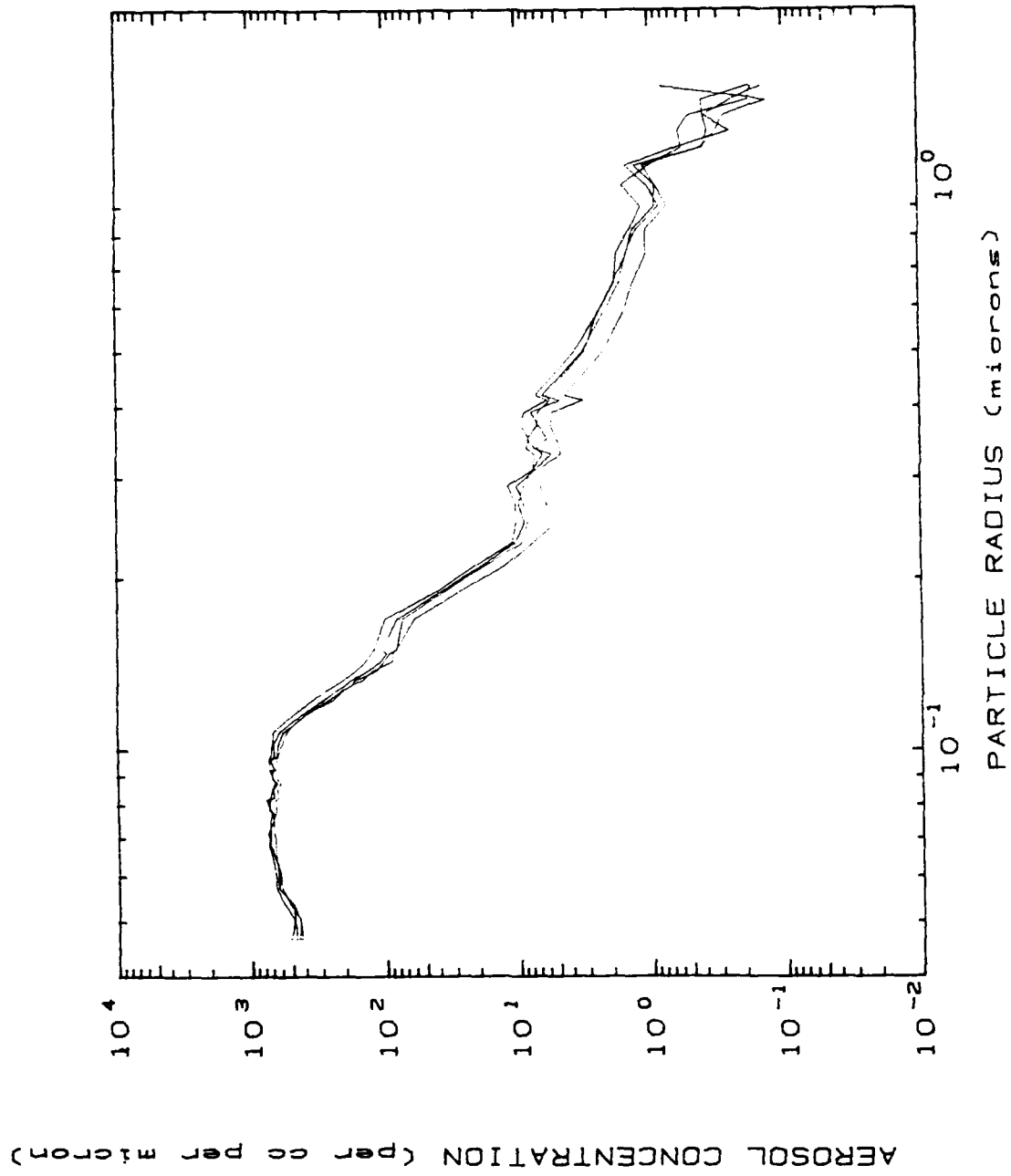
Fig. 12. Four consecutive data cycles of particle number concentration per cc per micron as a function of particle radius.
Mace Head, 10 March 1938.   Time: 1805-2120.   Wind direction: westerly.
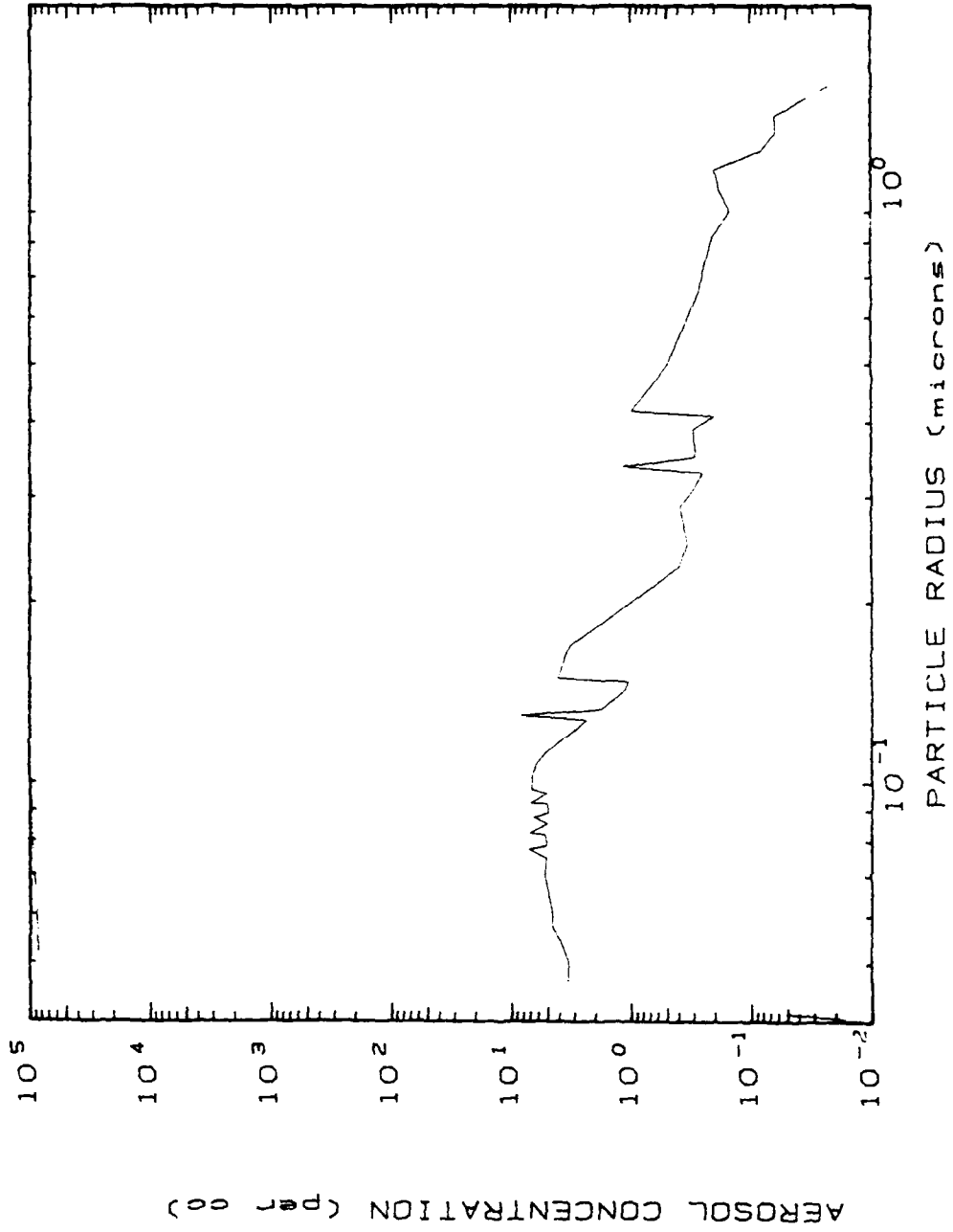
Fig. 13. A. average of the cyclic data shown in Fig. 11.
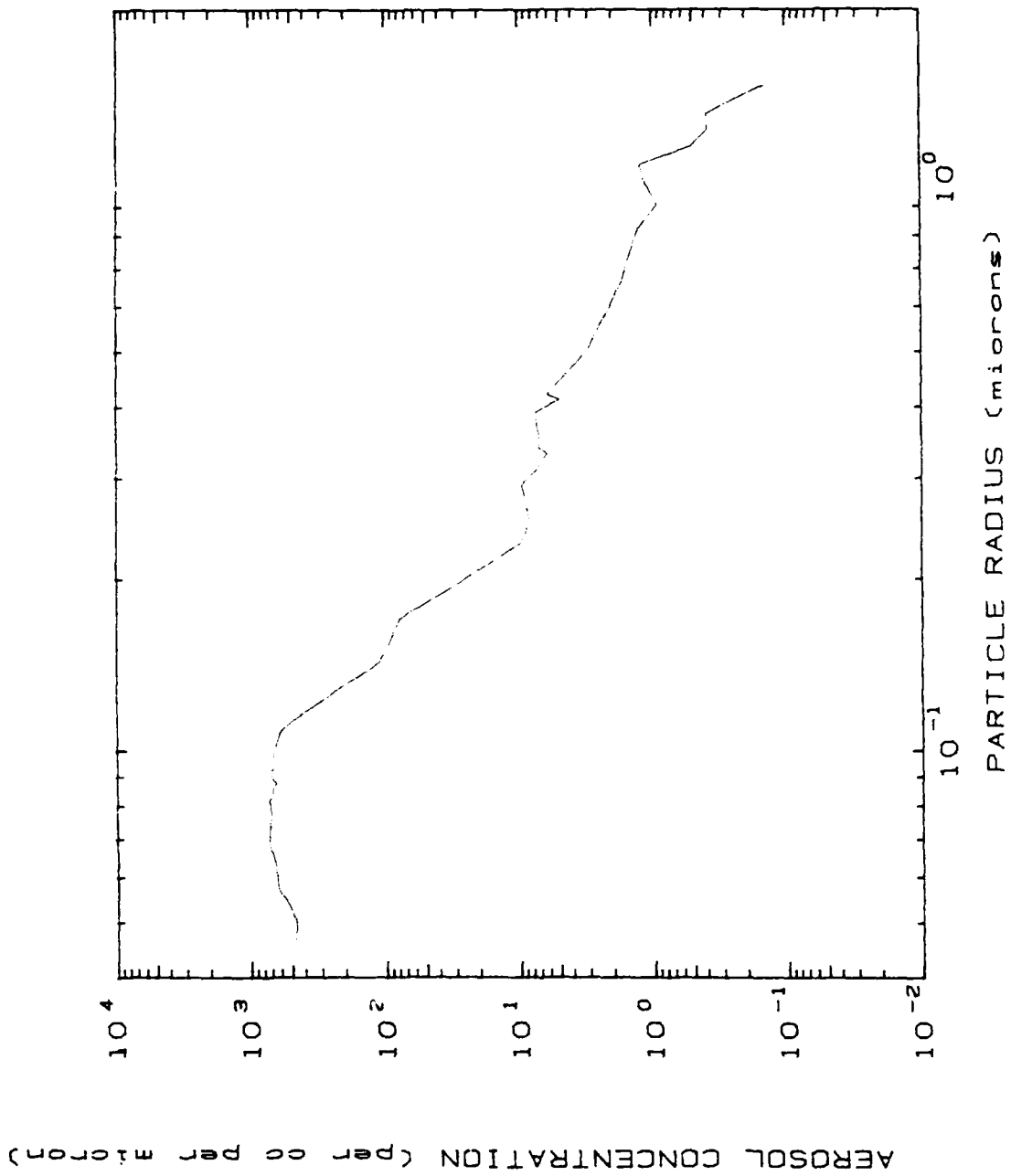
Fig. 14. An average of the cyclic data shown in Fig. 12.
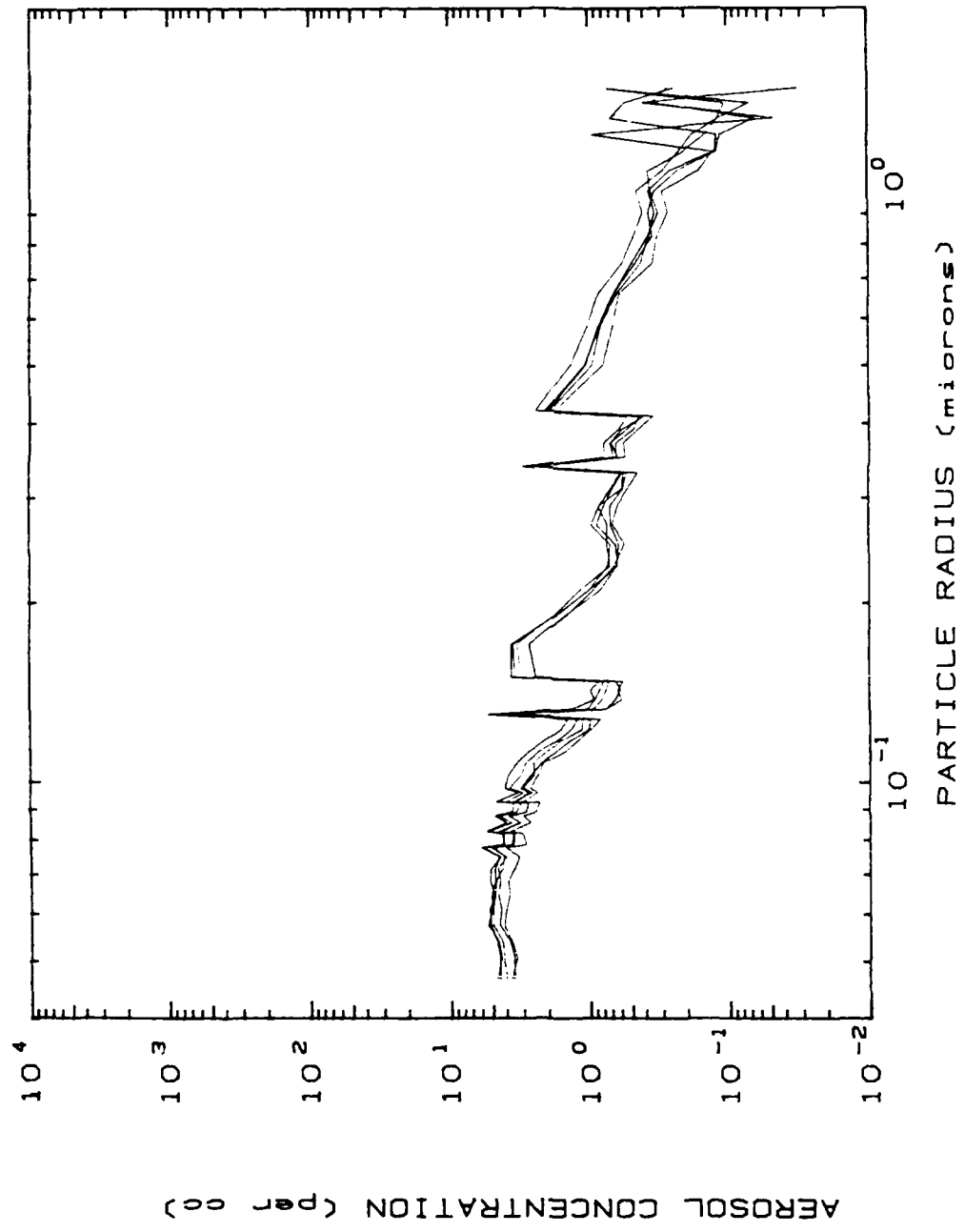
Fig. 15. Five consecutive data cycles of particle number concentration per cc as a function of particle radius.
Mace Head, 10-11 March 1988. Time: 2230-0235. Wind direction: west south westerly.

PARTICLE RADIUS (microns)

AEROSOL CONCENTRATION (per cc per micron)
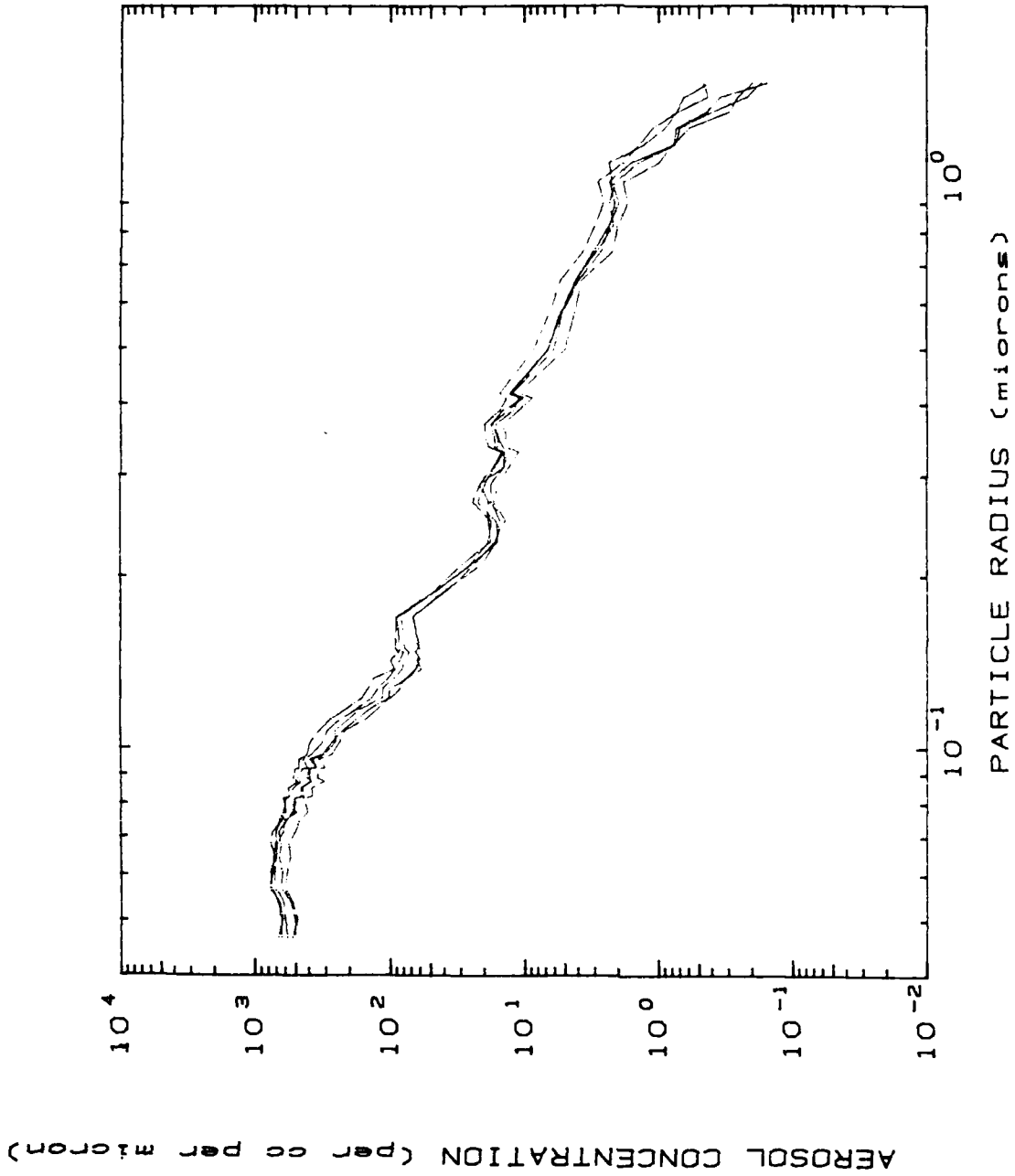
Fig. 16. Five consecutive data cycles of particle number concentration per cc per micron as a function of particle radius. Mace Head, 10-11 March 1988. Time: 2230-0235. Wind direction: west south westerly.
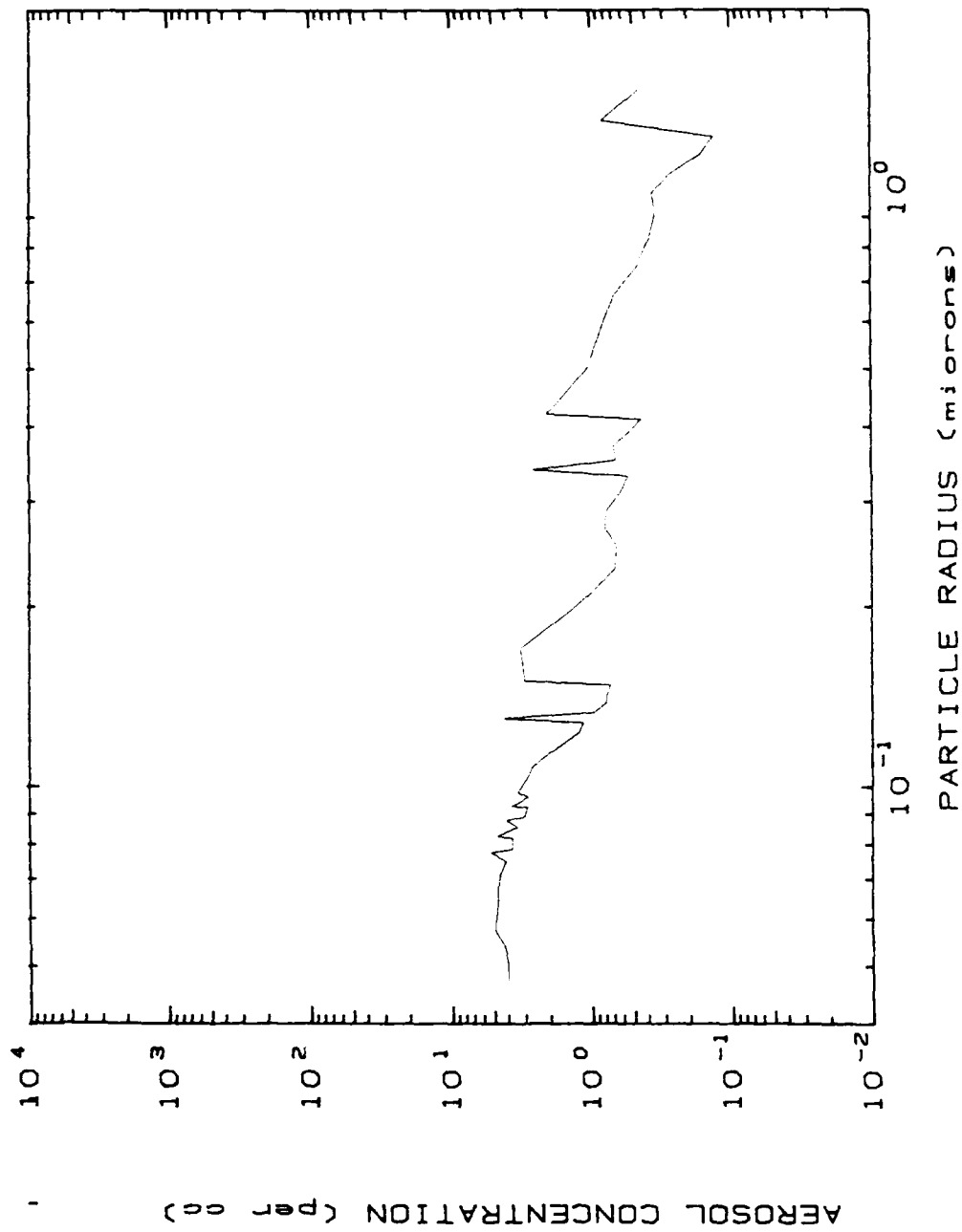
Fig. 17.   An average of the cyclic data shown in Fig. 15.

AEROSOL CONCENTRATION (per cc per micron)

PARTICLE RADIUS (microns)
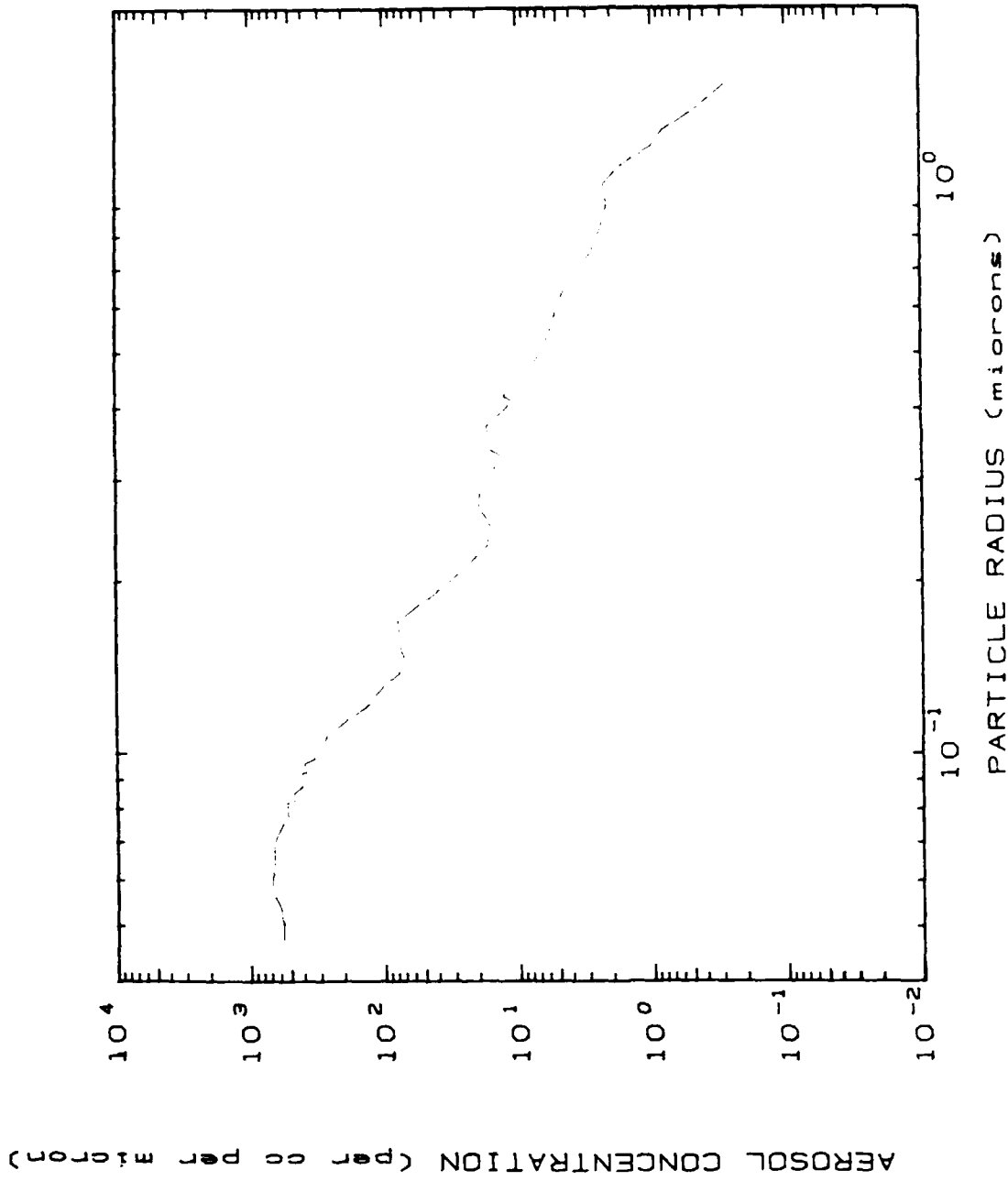
Fig. 18.   An average of the cyclic data shown in Fig. 16.

EXTINCTION COEFFICIENT (per m per micron)

PARTICLE RADIUS (microns)

10^{-1} 10^{0}

1.0^{-3} 10^{-4} 10^{-5} 10^{-6} 10^{-7} 10^{-8} 10^{-9} 10^{-10} 10^{-11} 10^{-12} 10^{-13}

WAVELENGTH

0.55 microns
0.6934 microns
1.06 microns
3.8 microns
10.6 microns
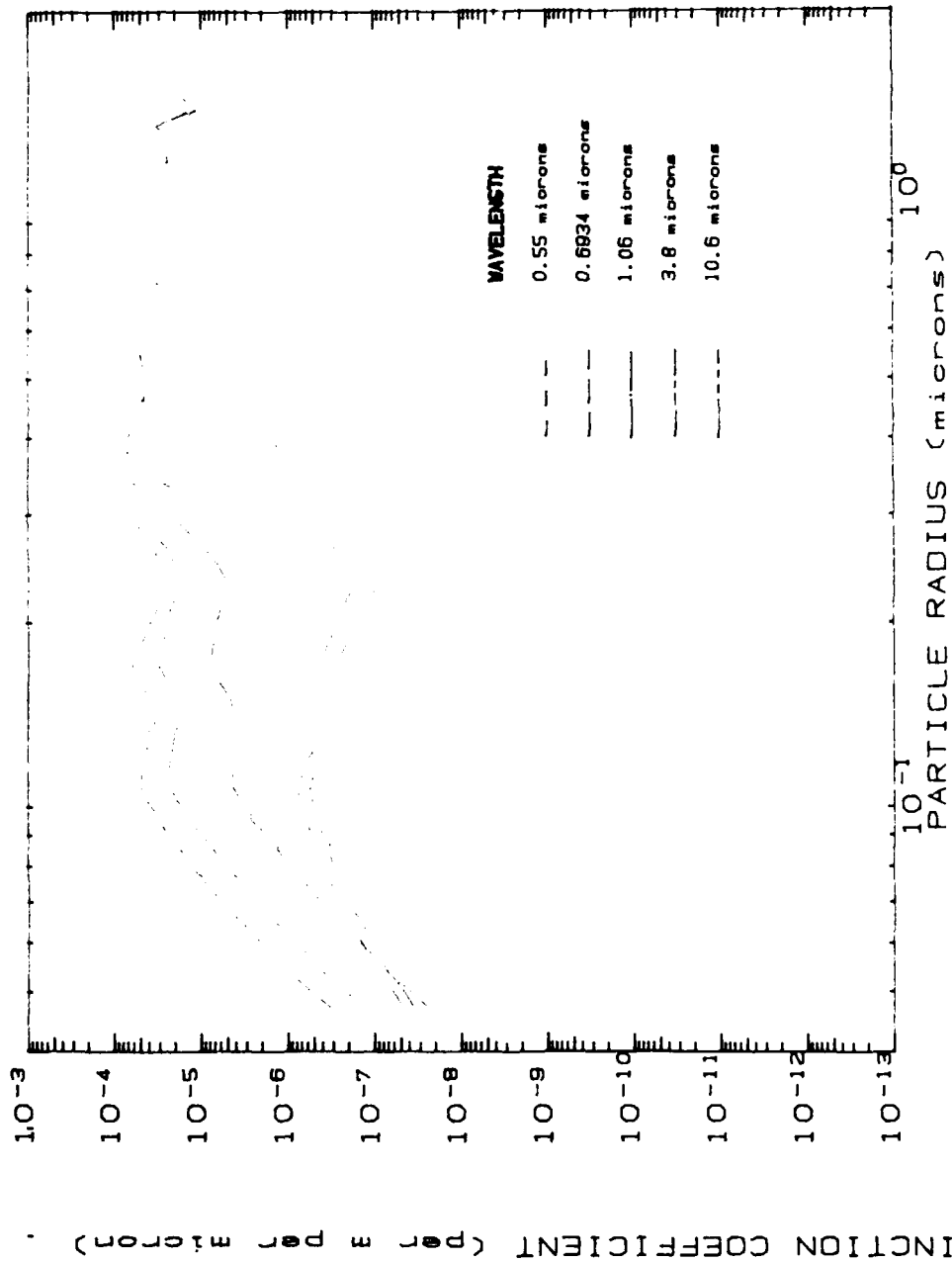
Fig. 19. Differential extinction coefficient per m per micron as a function of particle radius and wavelength based on averaged particle size distribution for the period 1805-2120, March 10th, 1988. Constituent: Ammonium sulphate.
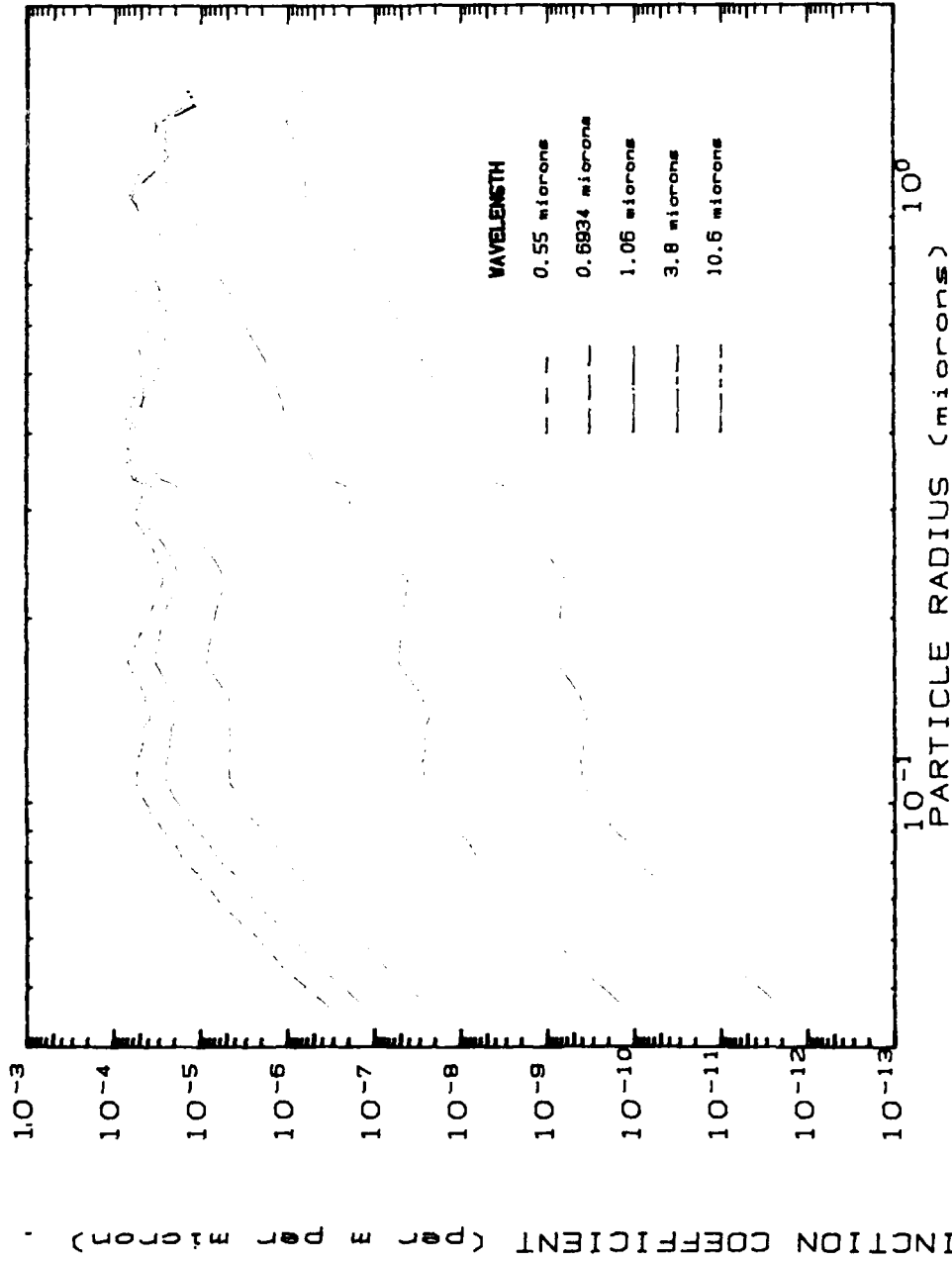
Fig. 20. Differential extinction coefficient per m per micron as a function of particle radius and wavelength based on averaged particle size distribution for the period 1805–2120, March 10th, 1988. Constituent: Sodium chloride.
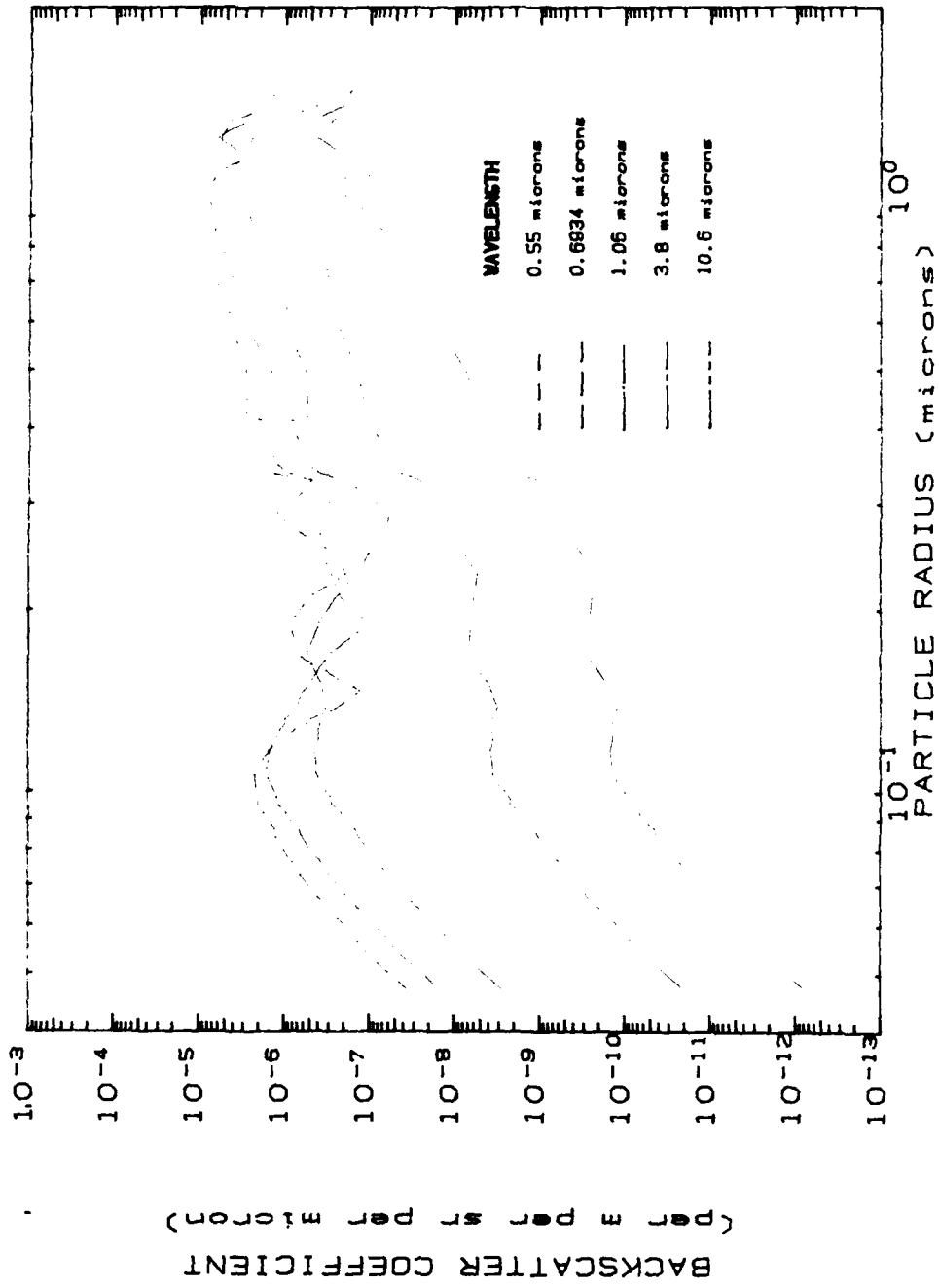
Fig. 21.   Differential backscatter coefficient per m per sr per micron as a function of particle radius and wavelength based on averaged particle size distribution for period 1805-2120, March 10th, 1988.   Constituent: Ammonium sulphate.
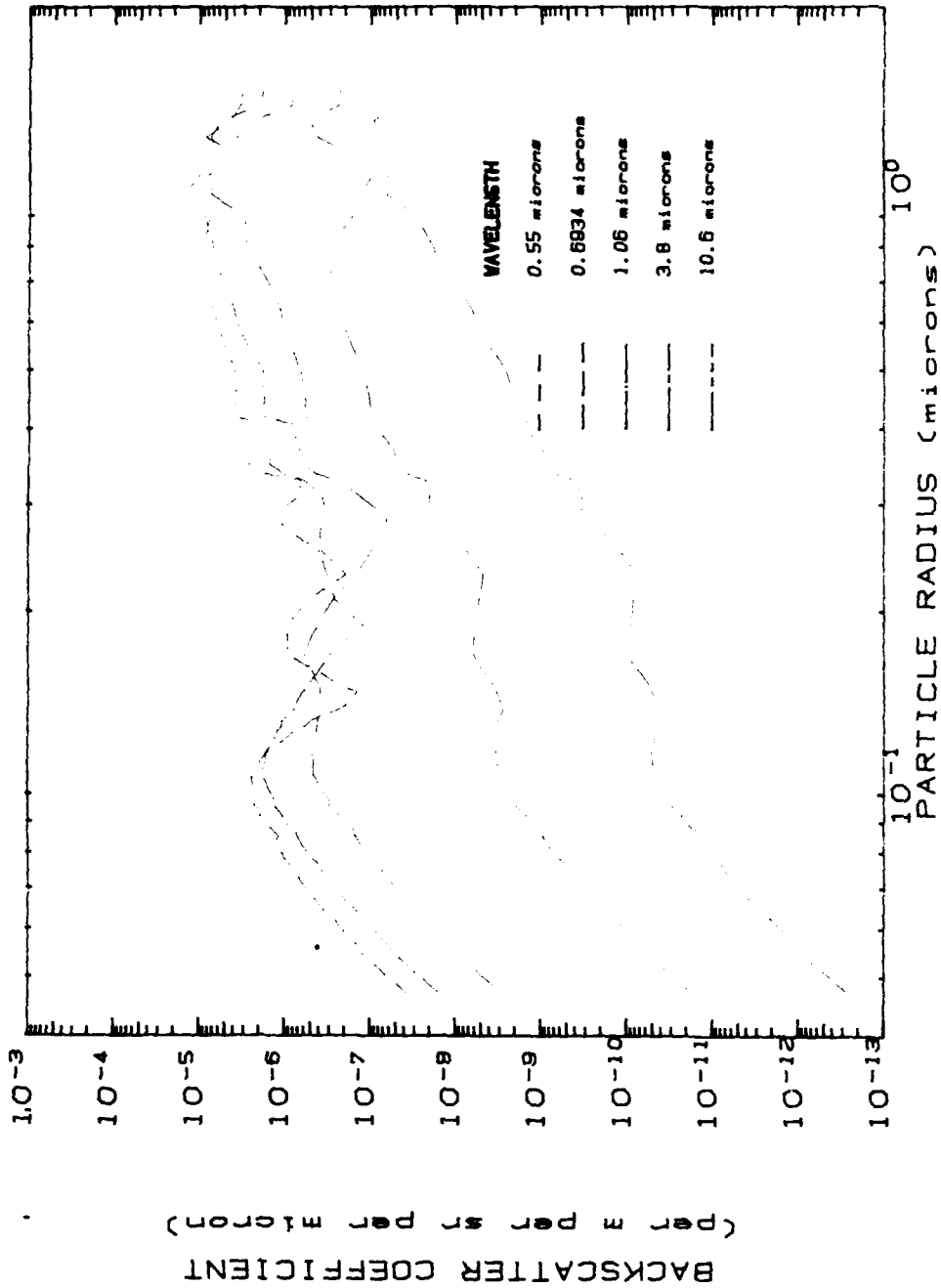
Fig. 22. Differential backscatter coefficient per m per sr per micron as a function of particle radius and wavelength based on averaged particle size distribution for period 1805-2120, March 10th, 1988. Constituent: Sodium chloride.

Fig. 23. Differential extinction coefficient per m per micron as a function of particle radius and wavelength based on averaged particle size distribution for period 2230-0235, March 10th-11th, 1988. Constituent: Ammonium sulphate.

EXTINCTION COEFFICIENT (per m per micron)

10-3 10-4 10-5 10-6 10-7 10-8 10-9 10-10 10-11 10-12 10-13

WAVELENGTH

0.55 microns
0.6934 microns
1.06 microns
3.8 microns
10.6 microns

10-1   10⁰
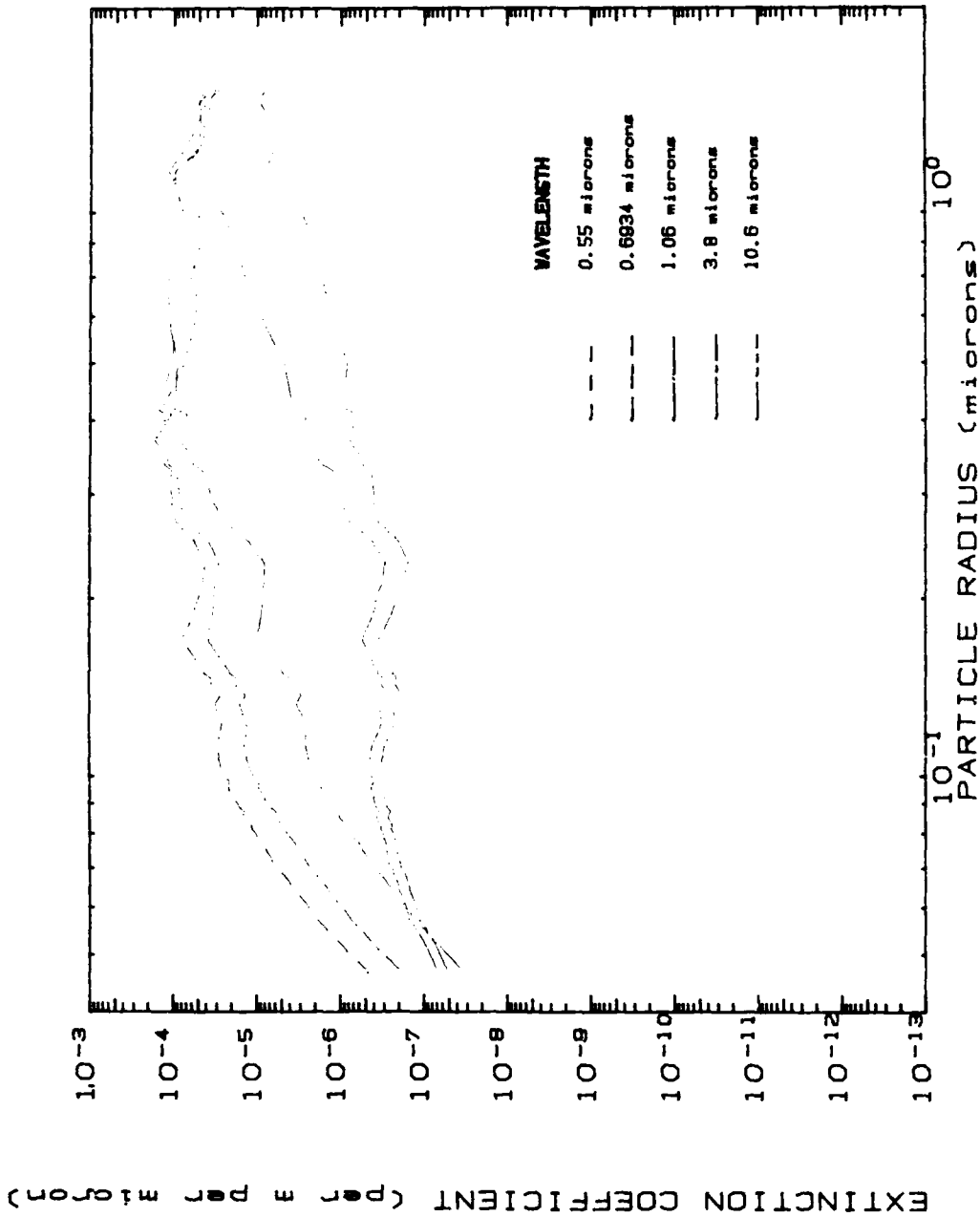
PARTICLE RADIUS (microns)
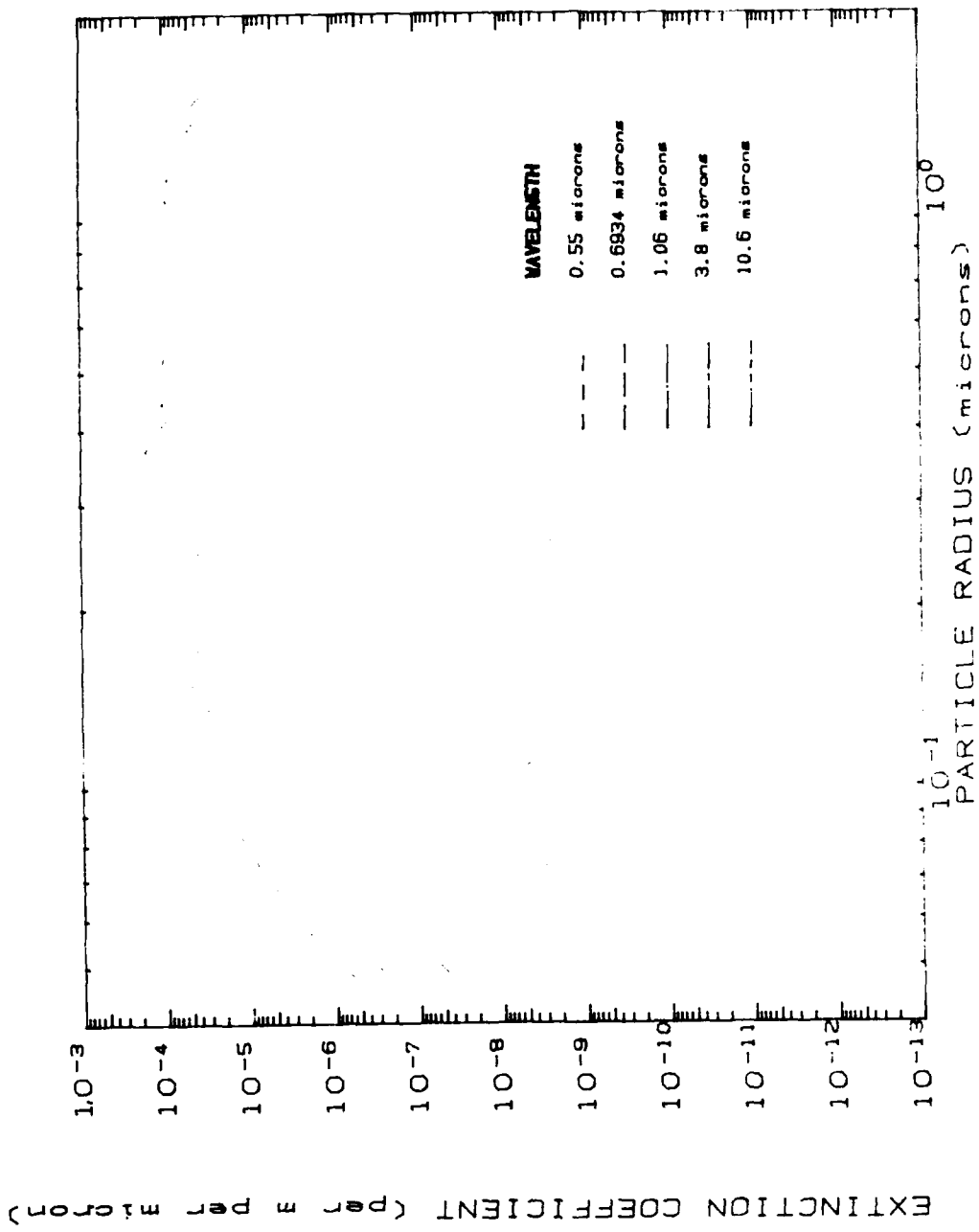
Fig. 24.   Differential extinction coefficient per m per micron as a function of particle
radius and wavelength based on averaged particle size distribution for period
2230-0235, March 10th-11th, 1988.   Constituent: Sodium chloride.
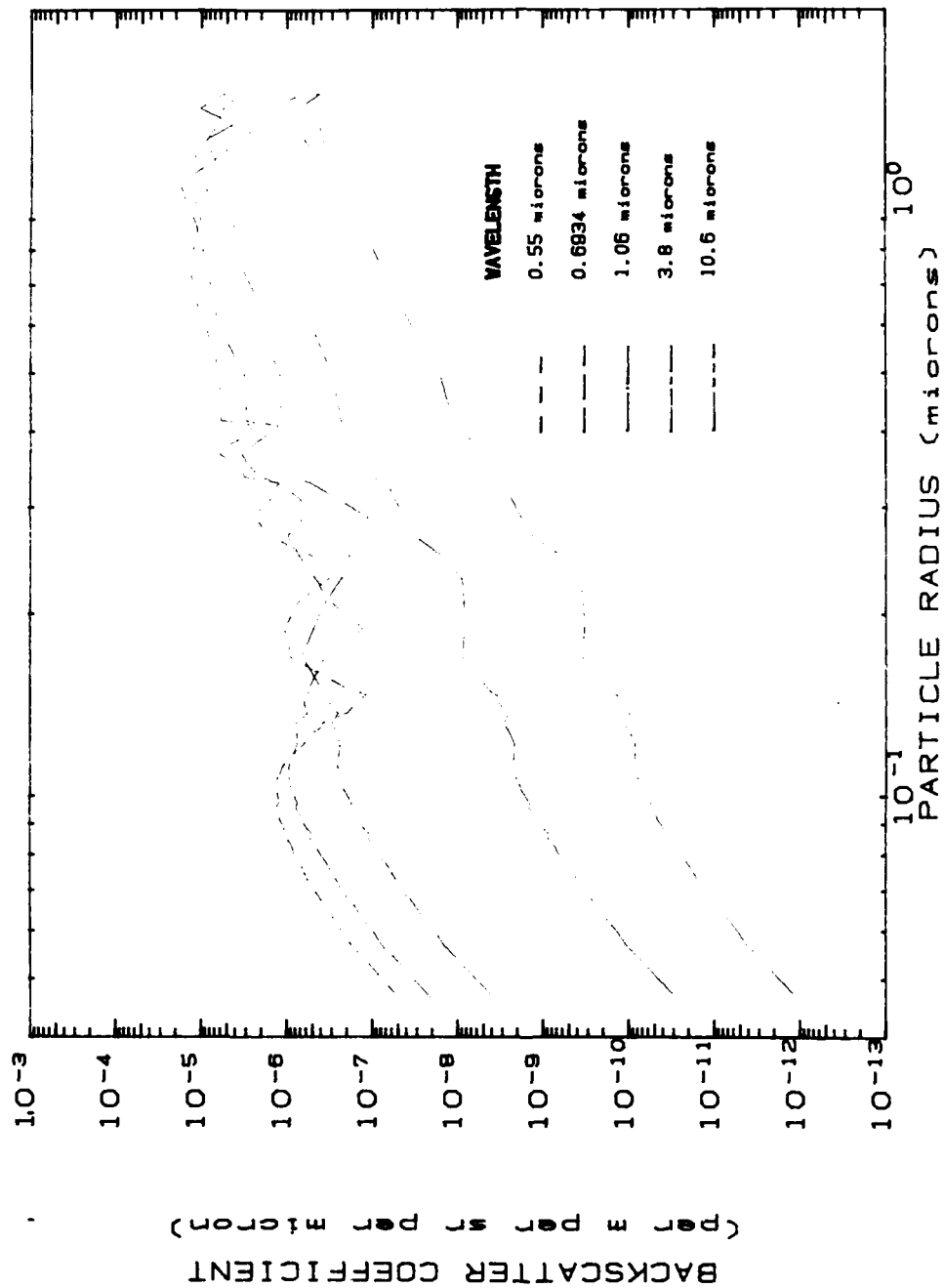
Fig. 25. Differential backscatter coefficient per m per sr per micron as a function of particle radius and wavelength, based on averaged particle size distribution for period 2230-0235, March 10th-11th, 1988. Constituent: Ammonium sulphate.
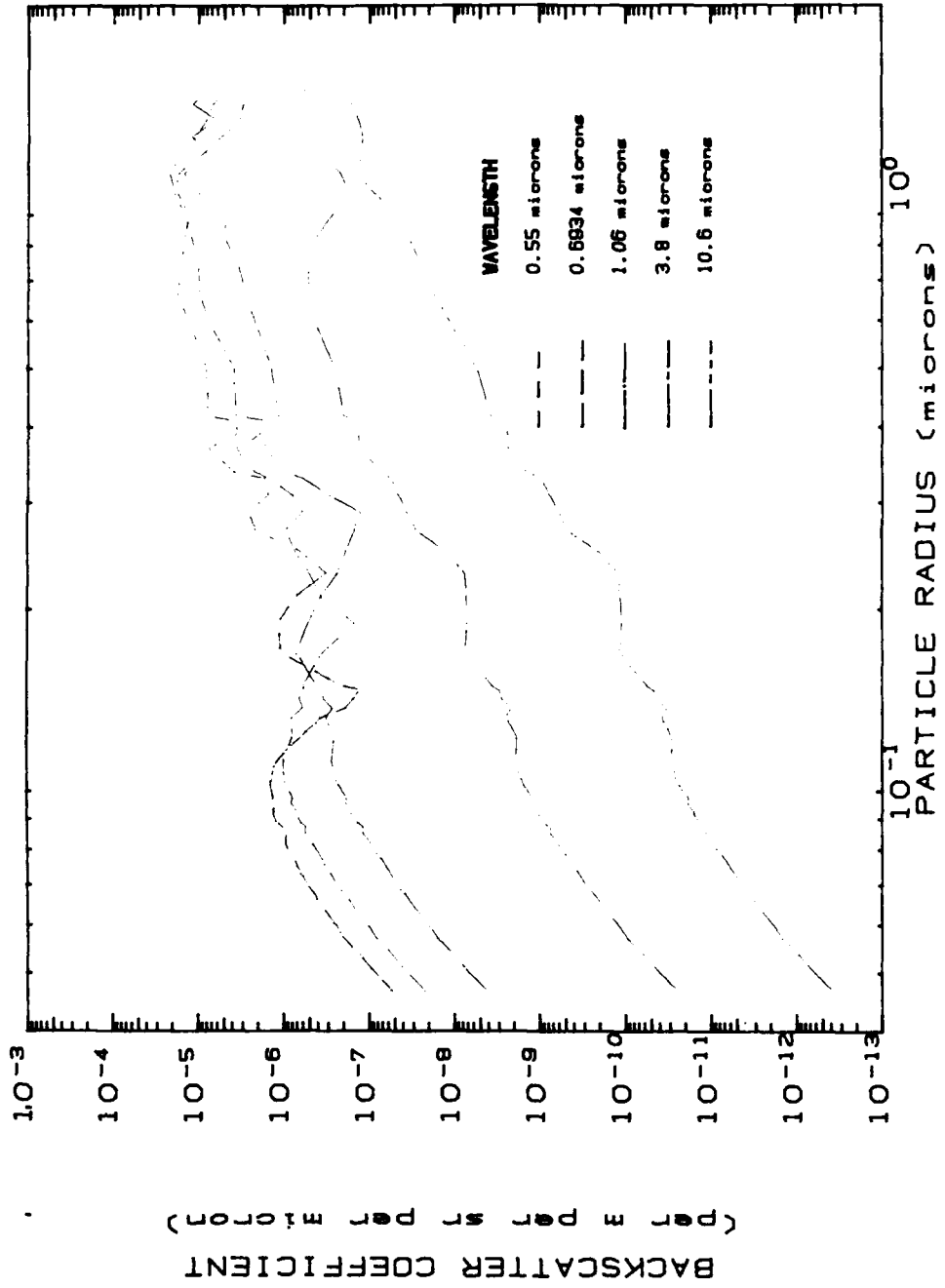
Fig. 26. Differential backscatter coefficient per m per sr per micron as a function of particle radius and wavelength, based on averaged particle size distribution for period 2230-0235, March 10th-11th, 1988. Constituent: Sodium chloride.
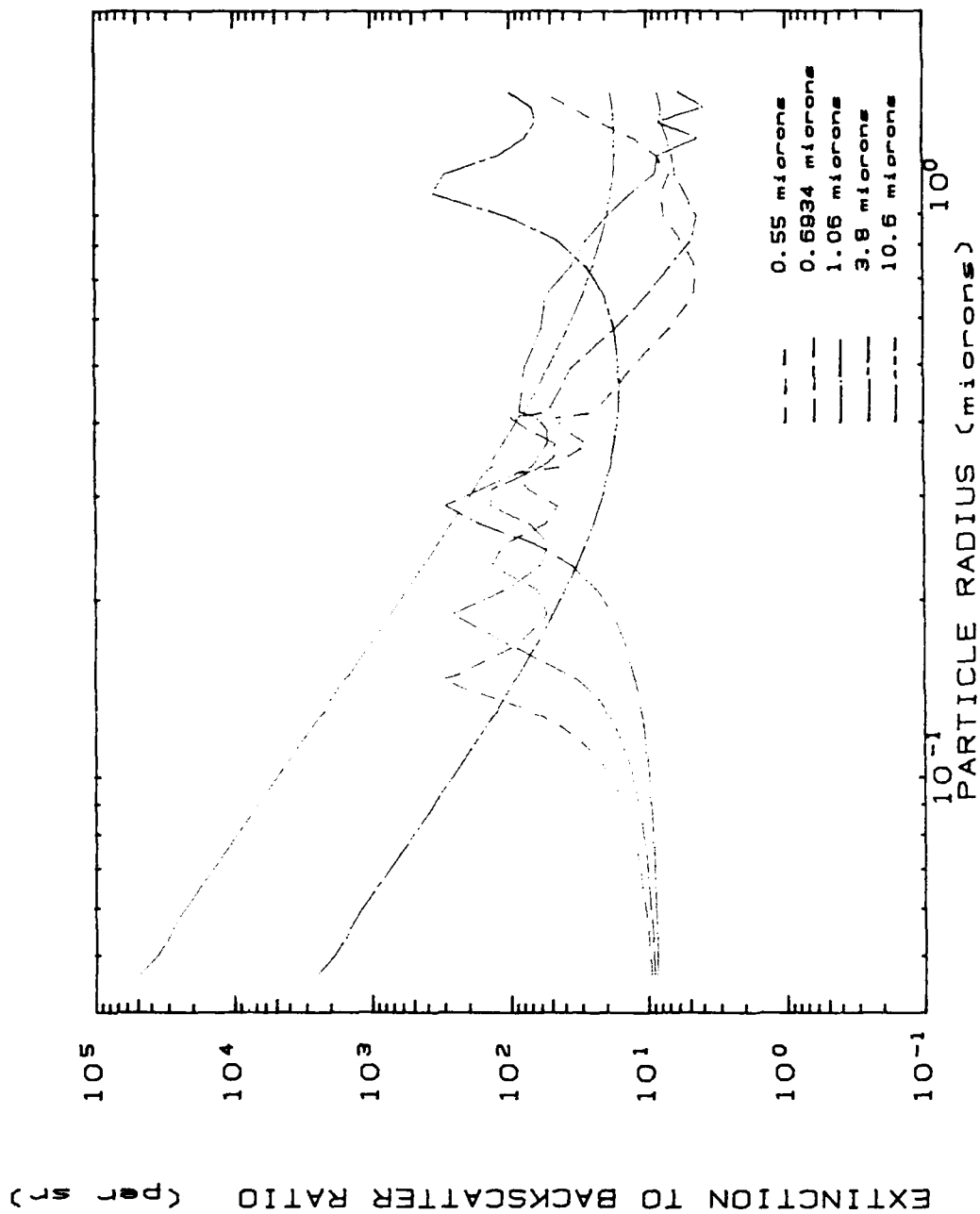
Fig. 27. Extinction to backscatter ratio per sr as a function of particle radius and wavelength. Constituent: Ammonium sulphate.
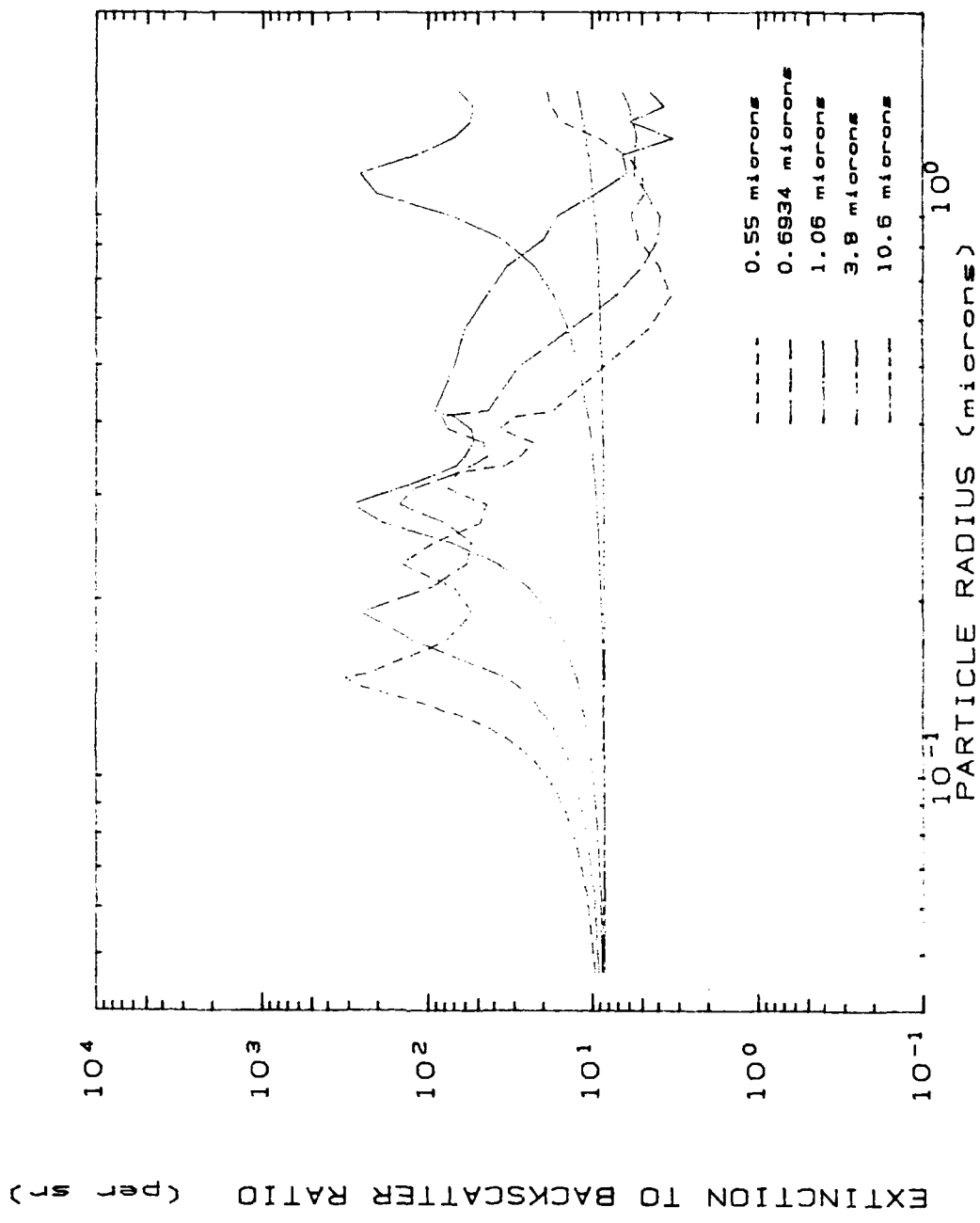
Fig. 28. Extinction to backscatter ratio per sr as a function of particle radius and wavelength. Constituent: Sodium chloride.